

Extreme Weather and Climate Change in Vermont: Implications for VEC's Asset and Storm Planning



August 9, 2021 - For: Vermont Electric Power Company
Prepared by: Northview Weather LLC
Contact: Dr. Jay Shafer - jason.shafer@northviewweather.com

Executive Summary

This report describes how climate change may present itself through the behavior of weather systems and climate states and how these changes may affect the reliable operation of Vermont's electric grid through 2049. High confidence results show that Vermont's climate is warming and becoming wetter, both of which will likely continue to increase into the future. Warmer and wetter storm systems will generally produce storms that are more intense (not necessarily more frequent) and cause more power outage disruptions to the distribution system. Seasonal changes to the warm season show a widening of the summer into early fall, which is expected to continue. This warm season widening will have the effect of lengthening the fall storm season into early winter (over 50% of all power outage impacts occur October to December). Despite a warming climate, the winter season will remain cold enough to sustain wet snow and ice risks through 2049. Overall weather-produced distribution system outage impacts are expected to increase by approximately 6% through 2049.

The distribution system may be affected by more intense storm systems, in particular from wind storms related to inland tracking tropical storms/hurricanes, whose potential intensity will be stronger in a warmer climate. More extreme high temperatures will also tend to shift annual peak loads to summertime. There did not appear to be significant changes to seasonal or annual solar energy variability.

Heavy precipitation events are expected to continue to increase around twice as fast as annual precipitation. A higher frequency of heavy precipitation events may result in greater widespread flooding risks, especially during the fall season. More irregular precipitation patterns are also likely, potentially leading to more intense drought conditions. However, vegetation health and growth analysis show no clear or strong indications as to how temperature and precipitation changes may affect future tree health and growth. The results described in this report are consistent with other published literature and provide deeper insights into how resilience investments may improve future reliability with climate change pressures across Vermont.

1. Introduction

It has been well documented that Earth's climate system is undergoing its most dramatic change in several million years in response to man-made greenhouse gas emissions. Carbon dioxide concentrations are now 418 ppm (Keeling and Tans, 2021), which are the highest in at least 3 million years (Rae et al, 2021). The pace of climate change may seem slow to human memory, but significant heat energy is currently accumulating in the oceans and the atmosphere, and the long residence time of atmospheric carbon dioxide ensures that responses to climate change will continue for generations even with dramatic actions to reduce greenhouse gas emissions today. A critical target to reducing the global risks to climate change is to keep global warming at or below 1.5°C; this target requires global carbon dioxide emissions to be at zero around 2050 (IPCC 2018). Regardless of the collective global actions of emissions reductions, the impacts from global climate change on Vermont's electric grid through 2049 will likely not be mitigated; in other words, it is prudent to take local action and plan based on current trends and higher-end projections.

It has been well documented that risks related to climate change are increasing pressures on the safe and reliable operations of the electric grid (e.g., Pantelli and Mancarella 2015). Weather variability is the largest single contributing factor to the day-to-day safe and reliable operation of the electric grid. Weather-sensitive applications may include load management for predicting electricity demand, storm planning and response for power outages, and renewable energy (solar, wind, hydro) management. This report quantifies extreme weather risks related to power outages examining various weather hazards (wind, snow, and ice). Both climate variability (long-term base states such as annual precipitation), and extreme weather variability (individual storm behavior) are described. It has been said that weather plays on the climate stage, which is to say that changing climate base states tend to stack the cards or change the percentages of how extreme weather states may occur. For example, increased average annual precipitation is associated with an even higher frequency of extreme precipitation events. Vermont's hazard mitigation plan has identified water and related flooding as the greatest risk to statewide infrastructure (Vermont Emergency Management 2018); by contrast wind storms pose the most significant risk to electric grid operations.

The relationship between climate indicators and vegetation growth and health is also generally described. Seasonal variability of temperature and precipitation is a significant factor affecting tree health and growth (VanHoutven et al. 2019). Longer growing seasons associated with seasonal warming may yield higher growth rates if soil moisture conditions remain adequate for sustained growth. However, more irregular precipitation patterns may potentially constrain seasonal growth and stress tree health. There appears to be significant uncertainty around species change and migration (e.g., Wang et al. 2016) across the Northeast US, with any tree species makeup changes being relatively nominal through 2049.

The purpose of this report is to understand the potential risks from climate change to the safe and reliable operations of the electric grid. As electrification accelerates, understanding these changes and their potential risks are critical for identifying future investments needed to maintain reliability. Results from this report should be used to inform decisions that may be necessary to maintain electric grid reliability with the pressures of climate change.

2. Data and Methods

a) Historic dataset and downscaling

The ECMWF Reanalysis 5 ([ERA5](#)) dataset was utilized in conjunction with a downscaled version to examine extreme weather and climatic trends from 1980-2019. The ERA5 reanalysis dataset uses the European Integrated Forecast System, more commonly the European/Euro weather model, to rerun known observations as input and is considered best in class. The native resolution of the ERA5 is 30-km; a downscaled version was created at a resolution of 5km using the Weather Research and Forecasting (WRF) model version 4.1 (Skamarock et al., 2019). WRF is a state-of-the-art computational fluid dynamics model used by national meteorological centers, private industry, and academia around the world to produce weather forecasts and climate simulations. The model is open-source and maintained by the [National Center for Atmospheric Research](#) (NCAR), Air Force Weather Agency, National Centers for Environmental Prediction, and the meteorological community. Downscaled versions were shown to improve performance resolving extreme wind events, as well as deriving the precipitation phase (wet snow and freezing rain).

b) Climate Projections Modeling

Climate simulations span the period covering 1980 through 2049, with historic baseline from 1980 to 2019 and the climate simulations starting in 2020 and ending in 2049. Projections are compared against the 1980-2019 baseline period, to determine the changes in frequency and magnitude of extreme weather events and seasonal climatic changes.

The projections use the WRF to downscale the Community Earth System Model version 1 (CESM). The CESM is a global climate model run by NCAR for the various Representative Concentration Pathways (RCP) scenarios. This work examined two climate scenarios representative concentration pathways from RCP8.5 (business as usual) and RCP4.5 (moderate emission curtailment) scenarios as initial conditions. NCAR has bias corrected the [CESM1](#) output using the ERA-Interim dataset (the precursor to the ERA5). The native resolution of the CESM data is 1.0 degree and is downscaled to 5km on an hourly basis for this work.

i) Domain Setup and Runtime Settings

The WRF domains used a parent domain of 25-km and a single nest of 5-km as described in Figure 1.

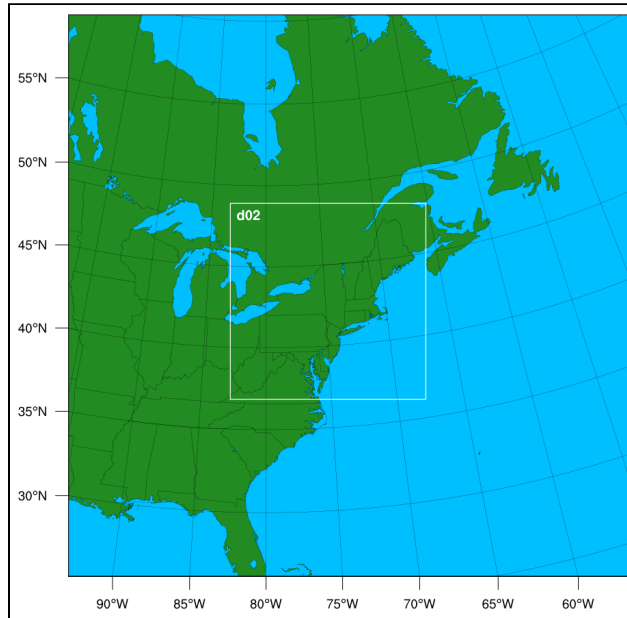


Figure 1. Regional climate model domain setup. The domains are a 25-5-km two-way nested setup. The 25-km domain matches the map boundary, while the 5-km domain is represented by the white bounding box.

ii) Model physics and dynamics options

The following model physics options were selected as shown in Table 1.

| Physical Process | Physics Option Selected |
|--------------------------|---------------------------------|
| Land Surface | Noah LSM (Tewari et al. 2004) |
| Surface Layer Physics | MM5 (Jimenez et al. 2012) |
| Planetary Boundary Layer | ACM2 (Pleim et al. 2007) |
| Cloud Microphysics | Thompson (Thompson et al. 2008) |
| Cumulus Parameterization | Kain Fritsch (Kain 2004) |
| Longwave Radiation | RRTM (Mlawer et al. 1997) |
| Shortwave Radiation | Dudhia (Dudhia 1989) |

Table 1. WRF model physics options used for downscaling.

In the WRF model configuration particular attention was given to the choice of planetary boundary layer and cloud microphysics for their impact on wind speed and precipitation

forecasting, respectively. The ACM2 planetary boundary layer scheme and MM5 surface layer scheme were selected based on work by Siuta et al. (2017), who found this scheme to have the highest accuracy of a number of schemes tested over complex terrain. For the cloud microphysics, the Thompson scheme was chosen for its superior fit to precipitation observations, notably in the wintertime when precipitation falls as snow (Thompson 2013; Lui et al, 2011). Settings for the Longwave Radiation, Shortwave Radiation, Noah LSM, and Cumulus Parameterization use the standard defaults for the WRF model.

Simulations were run a year at a time, starting at the beginning of fall (September 1). This allows the WRF model to adequately spin up its own snowpack/land cover/soil characteristics through the winter/spring months using the Noah land surface model physics. Throughout, the adaptive time stepping option was used to maximize numerical stability and runtime performance (speed of simulation). The process described in Bruyere et al. (2015) is followed with regards to the sea surface update settings.

iii) **Climate Simulation Limitations**

Climate simulations were limited to two high resolution simulations given project budget and the high computing costs. These two simulations were able to capture general climatic or base-state annual and seasonal changes for multiple variables (temperature, precipitation, solar radiation, wet snow, ice, and gradient winds). However, there were limitations with resolving extreme events. This under-sampling of extreme events was most apparent with gradient wind events, which showed approximately 20% fewer high wind events than the historic baseline (Figure 2). Poor representation of discrete extreme storm events with downscaled climate simulations is a known challenge (e.g., Seneviratne et al. 2012). In the simulations presented within this work mid latitude storm systems don't produce adequately strong storm systems and associated pressure gradients resulting in fewer high wind events. In contrast, however, precipitation variables did not feature the same underprediction.

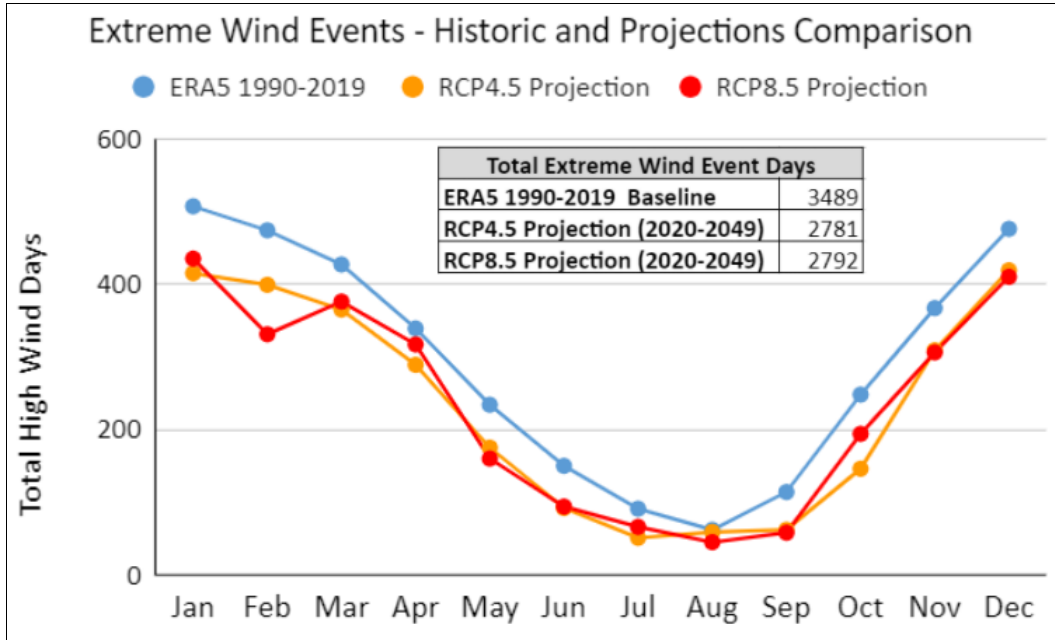


Figure 2. Vermont gradient wind frequency baseline and climate simulations.

iv) Trend Analysis and Hazard Climatology

The ERA5 30km dataset was used for most of the historical references of precipitation with the exception of wind gusts and aggregated rasters which used the downscaled ERA5 5km dataset. For the trends analysis hourly ERA5 rasters would be averaged (or the max or min would be found) to derive the daily summation. A spatial average would be composed upon a particular area (such as Vermont) which in turn would average all the grid boxes in the area of interest; as long as the outline of the area was in a grid box that grid box would be included. A daily time series was developed from these daily spatial averages in order to produce the trend analysis. The daily rasters were used once again to produce a hazard climatology. A threshold was chosen for each raster and they were added together to get a raster of frequencies for a time period.

v) Historical Outage Reconstruction and Deep Learning Model

Historical power outage data on the distribution system was provided by Vermont Electric Cooperative (VEC) from 2011 to 2019. Outage events and duration (in hours) were aggregated on a daily basis. Root cause was provided by VEC but it was difficult to isolate weather-caused outages vs non-weather events based on inconsistent reporting. In order to reconstruct historic outages, a deep learning model was developed using the 20 variables described in Table 2. Most weather variables were from the ERA5 30km, except for 24 hour peak wind gusts which were from the 5km downscaled ERA5. Incorporation of 48 hour precipitation accumulation allowed weather events of longer duration to be captured. The deep

learning model featured a mean absolute error of approximately 24 power outages a day (for reference the daily average number of events was 36).

| Variable//Feature | 24 Hour Duration | 48 Hour Duration |
|----------------------------------|------------------|------------------|
| Month | - | - |
| Day of Year | - | - |
| Precipitation | X | X |
| Rain | X | X |
| Ice Thickness | X | X |
| Snow | X | X |
| Wet Snow | X | X |
| Temperature | X | - |
| Dew Point | X | - |
| Mean Sea Level Pressure | X | - |
| Soil Moisture level 1 (0 - 7cm) | X | - |
| Soil Moisture level 2 (7 - 28cm) | X | - |
| Wind Gust | X | - |
| Leaf Area Index | X | - |
| Wind Directions (NW,W,NE...) | X | - |

Table 2. Variables (features) used to create historic outage data using a deep learning model.

Two deep learning models that were created; one using outage events and another using outage duration. Outage events and outage duration or label data (what is being solved for) were aggregated on a daily basis and therefore could be matched to the variables/features in Table 2. The data was then split into 80% training data and 20% test data. Both training and test datasets were standardized so the model would converge on a solution quicker during training. The training model had 3 layers with 64,32 and 1 neuron(s). The historical feature data covering the 1980-2019 time period was then inputted into the newly created model.

3. Climatic Trends

a) Temperature

i) Annual Temperature

Temperatures are steadily increasing. The average annual temperature aggregated across VEC's region from 1980-2019 was 42.8°F (Figure 3). The maximum annual temperature during this period was 45.4°F and the minimum was 40.8°F. The annual trend has been positive with a 1980-1999 average temperature of 42.4°F and a 2000-2019 average temperature of 43.2°F therefore making a difference of +0.8°F between time periods. This warming is consistent with regional and global warming (USGCRP 2018).

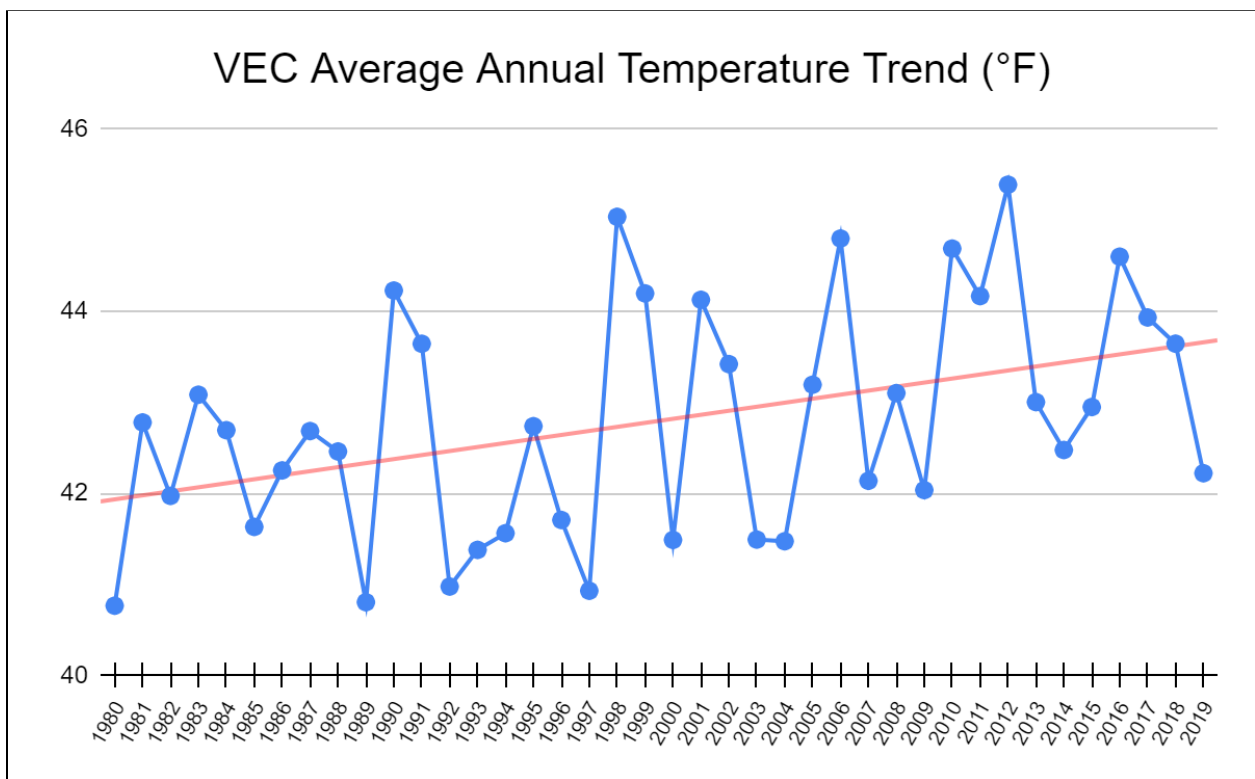


Figure 3. VEC region annual temperature trend from 1980-2019 based on 30-km ERA5.

ii) Seasonal Temperature

Seasonal temperature changes are not equally distributed across the year. Spring and fall temperatures exhibit average temperatures that are near the range of the average annual temperatures with 45.9°F in the fall and 41.0°F in the spring. Summer has an average temperature of 65.0°F and winter has an average temperature of 19.0°F. All seasons show warming as seen in Figure 4. The strongest seasonal warming occurs in the fall with a temperature change of +1.6°F between 1980-1999 and 2000-2019. This warming trend appears

to be associated with an elongation of the warm season into the fall season, with 3 out of the top four warming months being in the fall and late summer (not shown).

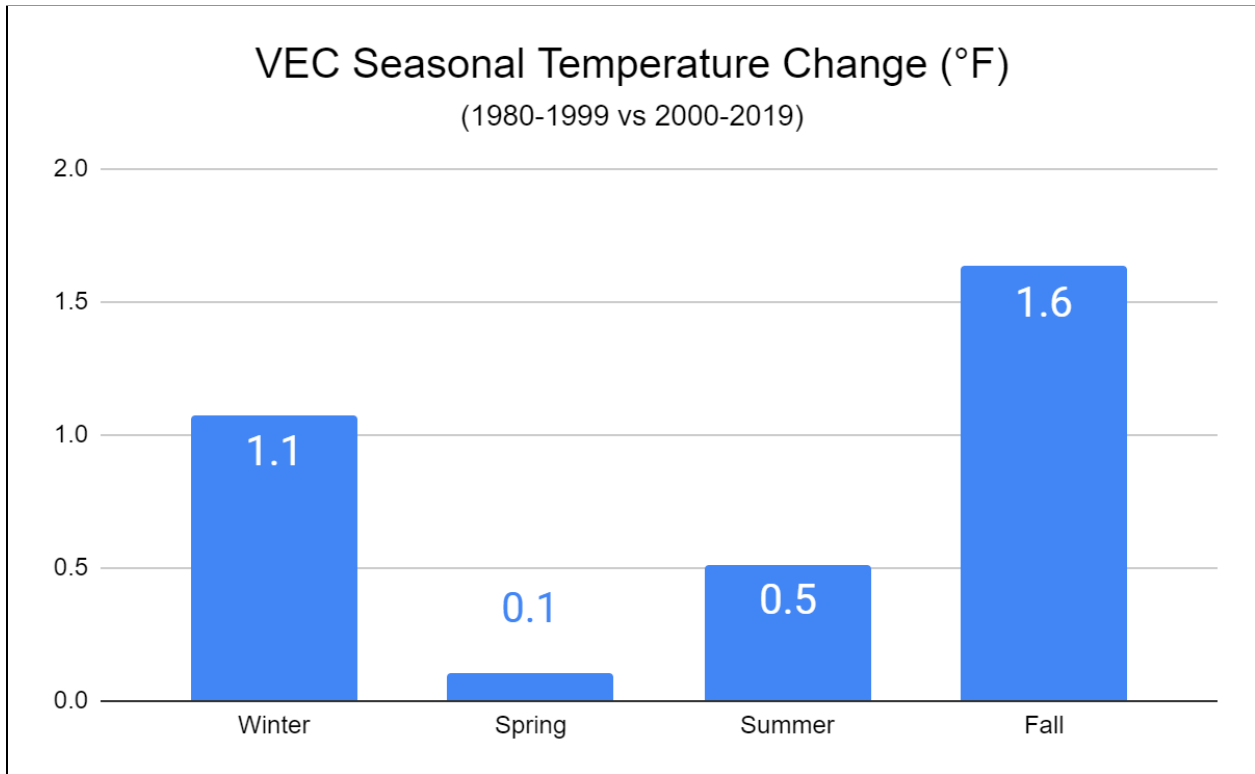


Figure 4. VEC region temperature change (°F) for each season between 1980-1999 and 2000-2019. Winter is Dec, Jan, Feb, Spring: Mar, Apr, May, Summer: Jun, Jul, Aug, Fall: Sep, Oct, Nov.

iii) Growing Degree Days

Warmer temperatures produce a longer growing season, at least as measured by growing degree days. Growing degree days are a measure of the accumulated heat energy and can be used to reference a variety of plant and tree species growth potential. There has been a steady increase in growing degree days from 1980 to 2019 (Figure 5). The average annual growing degree days from 1980-1999 was 1795 days while the average annual growing degree days from 2000-2019 was 1933 days, resulting in a 7.7% increase in growing degree days. The majority of this increase is due to a lengthening of the growing season in the late summer and early fall; not all plant and tree species may be able to realize this seasonal extension, as many tree species put up much of their seasonal growth in the first part of the growing season. Spring was shown to be a less reliable season despite a general earlier arrival of the growing season with colder temperatures being equally likely to linger or return after the first spring warm up.

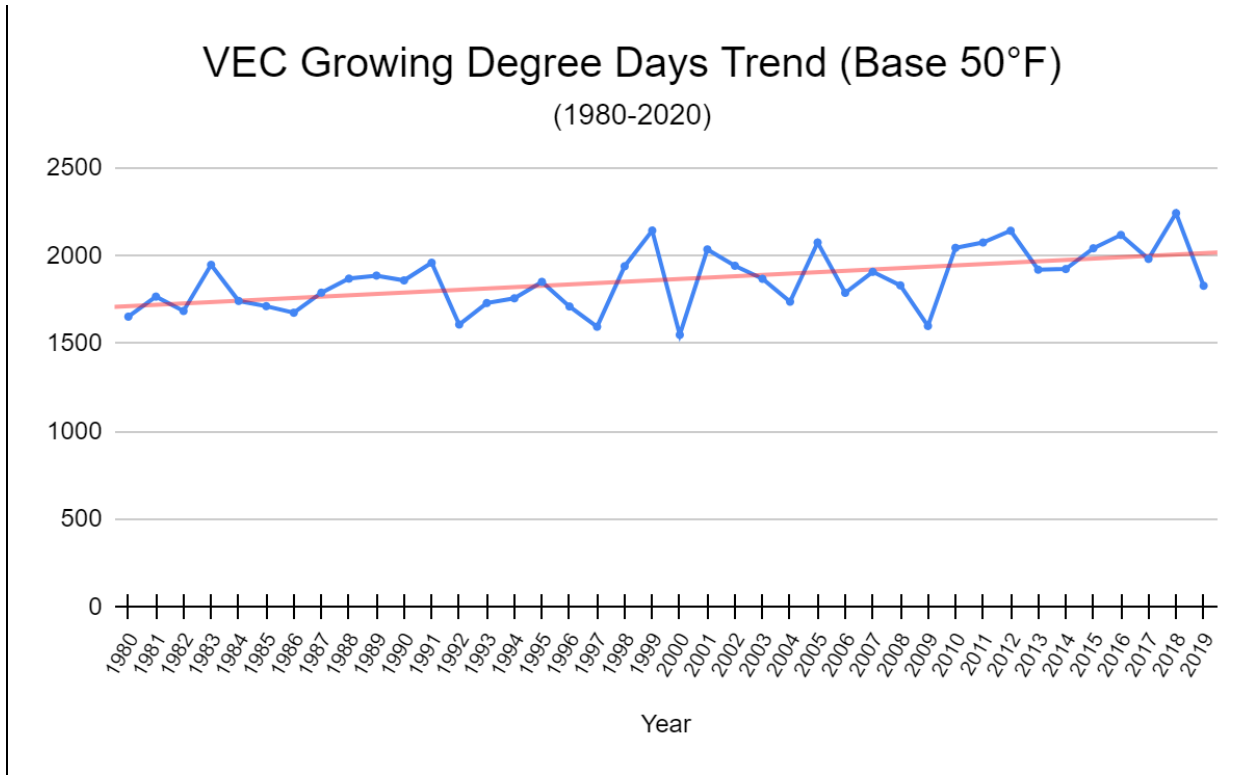


Figure 5. VEC region growing degree days trend with a base of 50°F for calculating growing degree days.

iv) Extreme Temperature Climatology and Trends - Heat

The spatial distribution of where temperatures reach above 80°F varies based on location and elevation (Figure 6). High elevations, locations near Lake Champlain, and northeasternmost Vermont have the lowest frequency of heat days while the deeper Champlain and Connecticut River Valleys experience the most. The warmest locations average approximately 35 days a calendar year above 80°F. Trends in heat days show an overall increase statewide, with the least number of increases at the highest elevations where temperatures remain below the 80°F threshold. However, the more rapid increases as percent show that middle elevations such as the Northeast Kingdom and Green Mountains are seeing more rapid warming as temperatures warm with elevation (Figure 7).

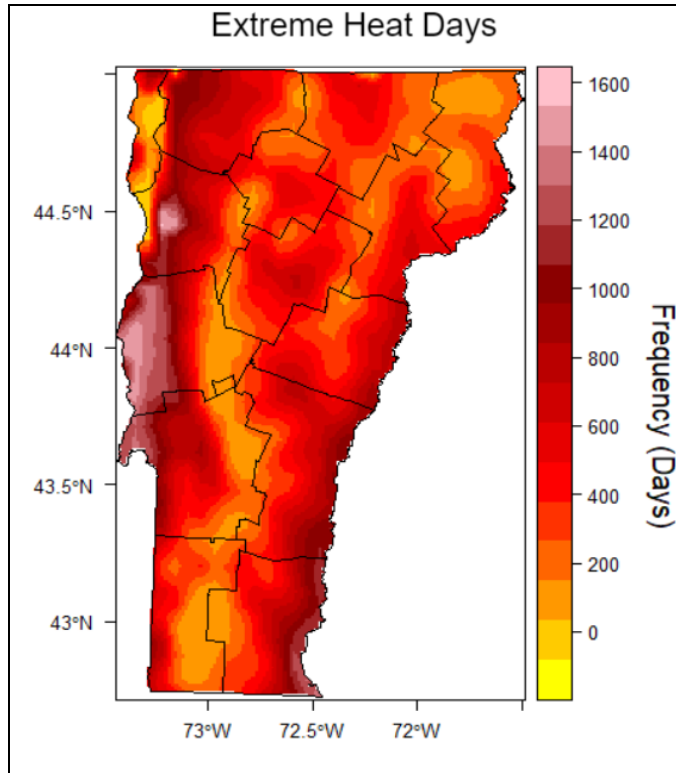


Figure 6. Extreme heat days as defined with a high temperature above 80°F in a 24 hour period per grid box during 1980-2019.

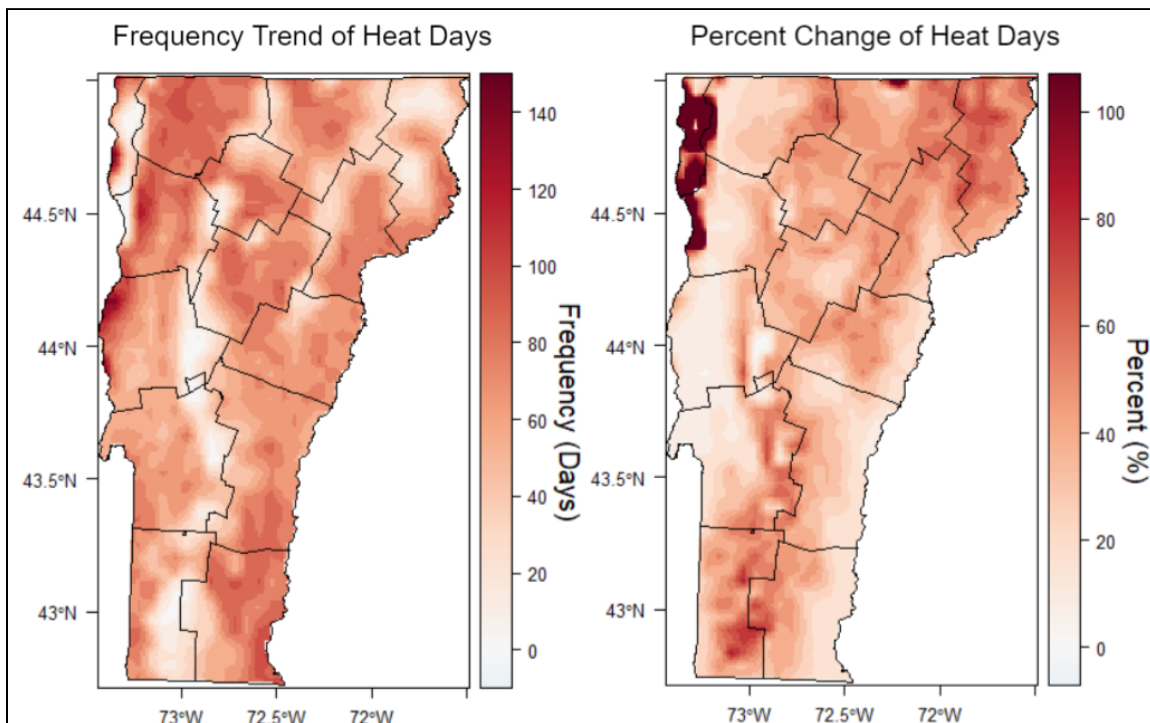


Figure 7. Extreme heat days (high temperature reached 80°F) frequency change from 1980-1999 to 2000-2019 (left) and percent change (right). Data based on downscaled ERA5 5km data.

v) Extreme Cold Temperature Climatology

Northeastern Vermont has the greatest amount of extreme cold days while locations near Lake Champlain have the least (Figure 8). The coldest locations approach 30-40 days a season with a low temperature at or below 0°F, whereas the warmest locations average closer to 10 days a winter. As elevation increases the amount of extreme cold days generally increases as well.

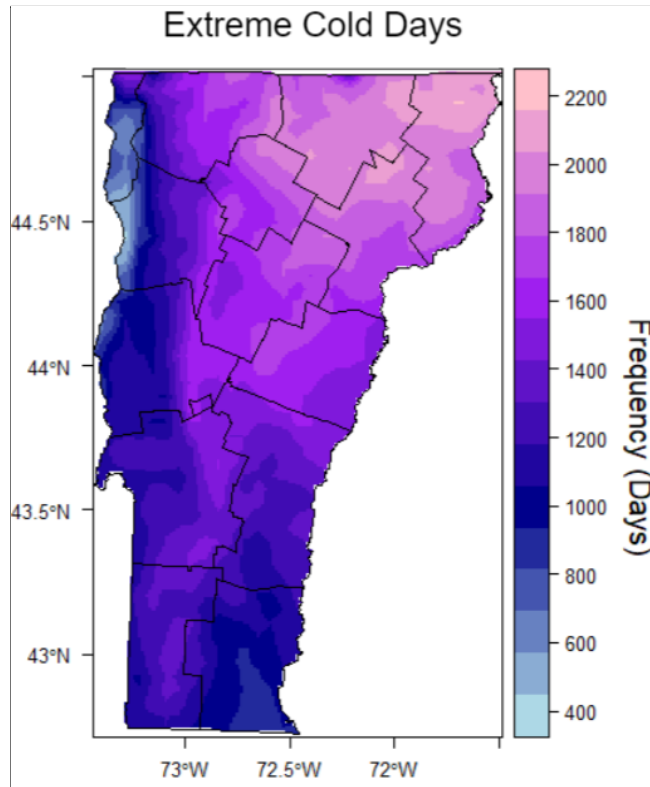


Figure 8. Extreme cold days as defined with a high temperature at or below 0°F in a 24 hour period from 1980-2019.

vi) Extreme Temperature Climatology and Trends - Cold

Extreme cold days have been decreasing throughout Vermont with about 1 to 3 fewer cold days a winter season as the 20-year trend (Figure 9). Northwestern Vermont has experienced the greatest decrease in extreme cold days as well as the greatest percentage decrease with relatively uniform spatial variability in other locations (Figure 9).

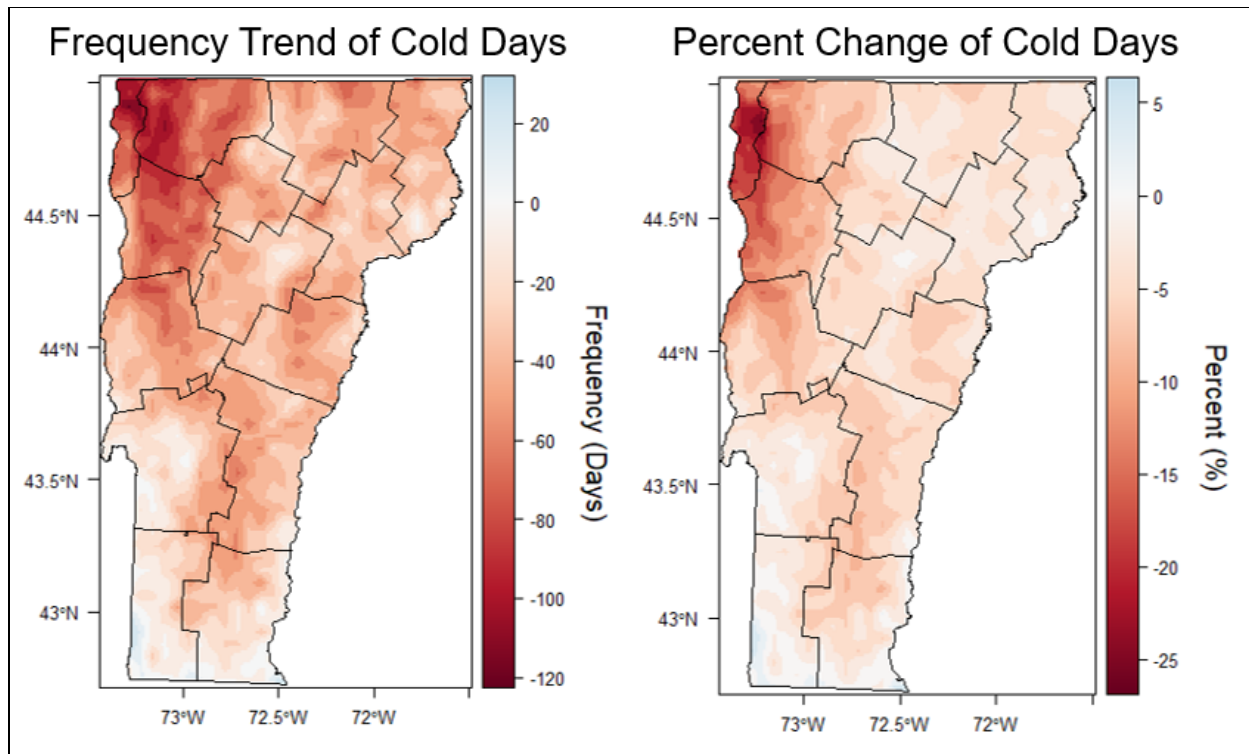


Figure 9. Difference in extreme cold days (days where minimum temperatures was below 0°F) between 1980-1999 to 2000-2019 (left). Percent increase or decrease in extreme cold days (days where minimum temperatures went below 0°F) between 1980-1999 to 2000-2019 (right).

b) Precipitation

i) Annual Precipitation

Precipitation is one of the most complex weather and climate variables whose formation depends on a variety of complex processes. At a simplified level precipitation formation in midlatitude climates such as Vermont depends on the availability of moisture, amount of upward motion (as driven by weather systems), and temperatures at which precipitation may grow within a cloud. More complex factors such as atmospheric stability, land-surface feedback processes (e.g., evaporation), track and movement of storm systems can also modulate precipitation formation.

VEC's area averages about 49.5 inches of precipitation per year (1980-2019). The maximum precipitation during this period was 57.9 inches in 1996 and minimum in 2001 with 37.7 inches (Figure 10). Vermont's climate has been relatively stable with respect to annual precipitation variability. Annual precipitation has a strong influence on tree species growth, with available soil water capacity being a key indicator of annual growth potential (Swanston et al, 2017). There has been an increasing trend of precipitation from 1980-1999 to 2000-2019 with an increase of approximately 1.8" resulting in an approximate 3.8% increase as the 20-year trend (Figure 10).

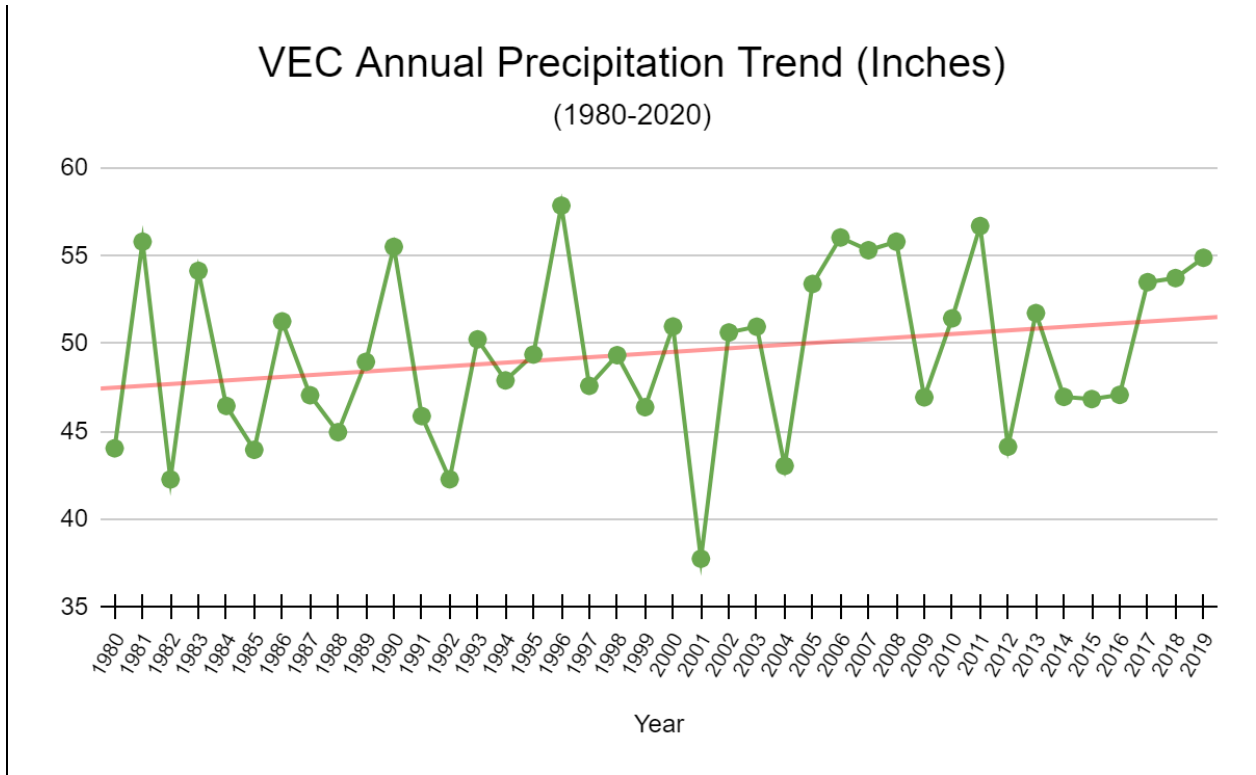


Figure 10. Annual precipitation (inches) across VEC region from 1980-2019 using the ERA5 30km dataset.

ii) Seasonal Precipitation and Trends

The summer produces the most precipitation although October has the third most rainfall (Figure 11). October’s maximum is likely related to a combination of midlatitude storm systems interacting with remnant moisture from tropical storms (e.g., Huang et al, 2017). Winter has seen the greatest increases in overall precipitation, with a 20-year increase of 10.3%, while there has been little change to spring and summer precipitation (Figure 12).

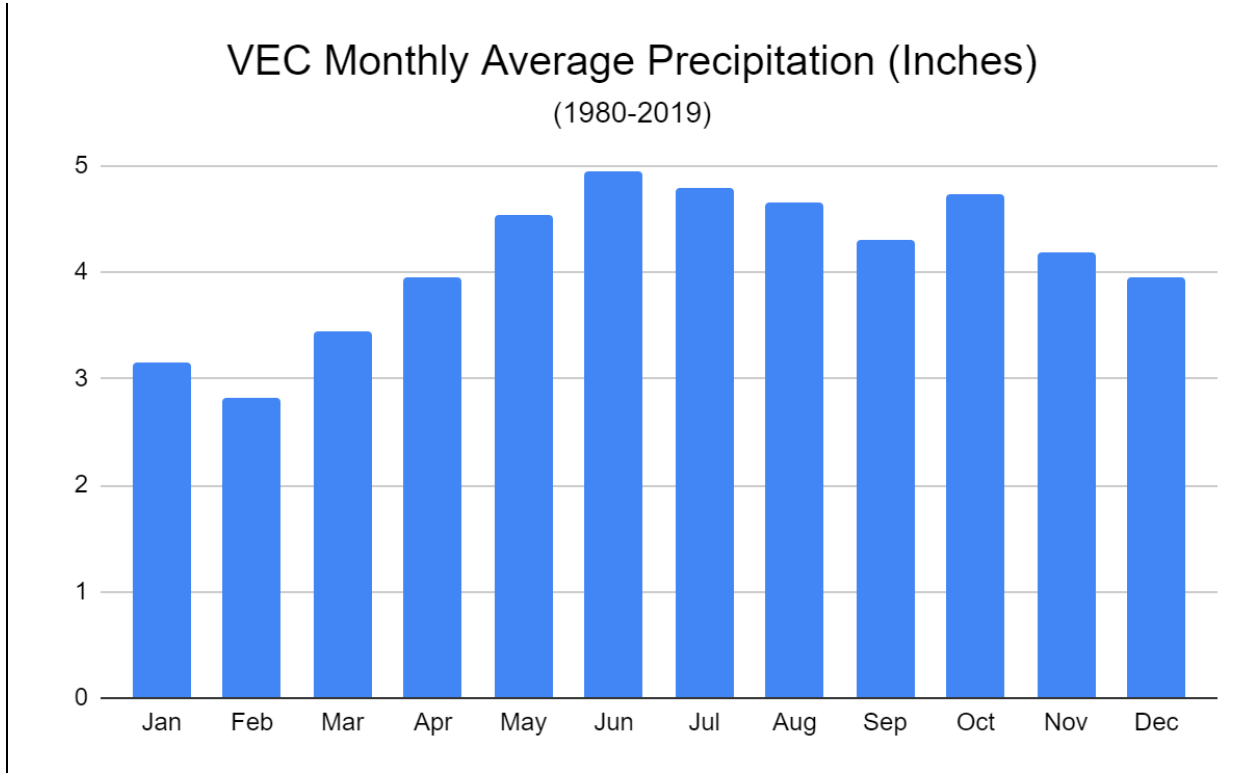


Figure 11. VEC monthly precipitation (inches) using the ERA5 30km reanalysis.

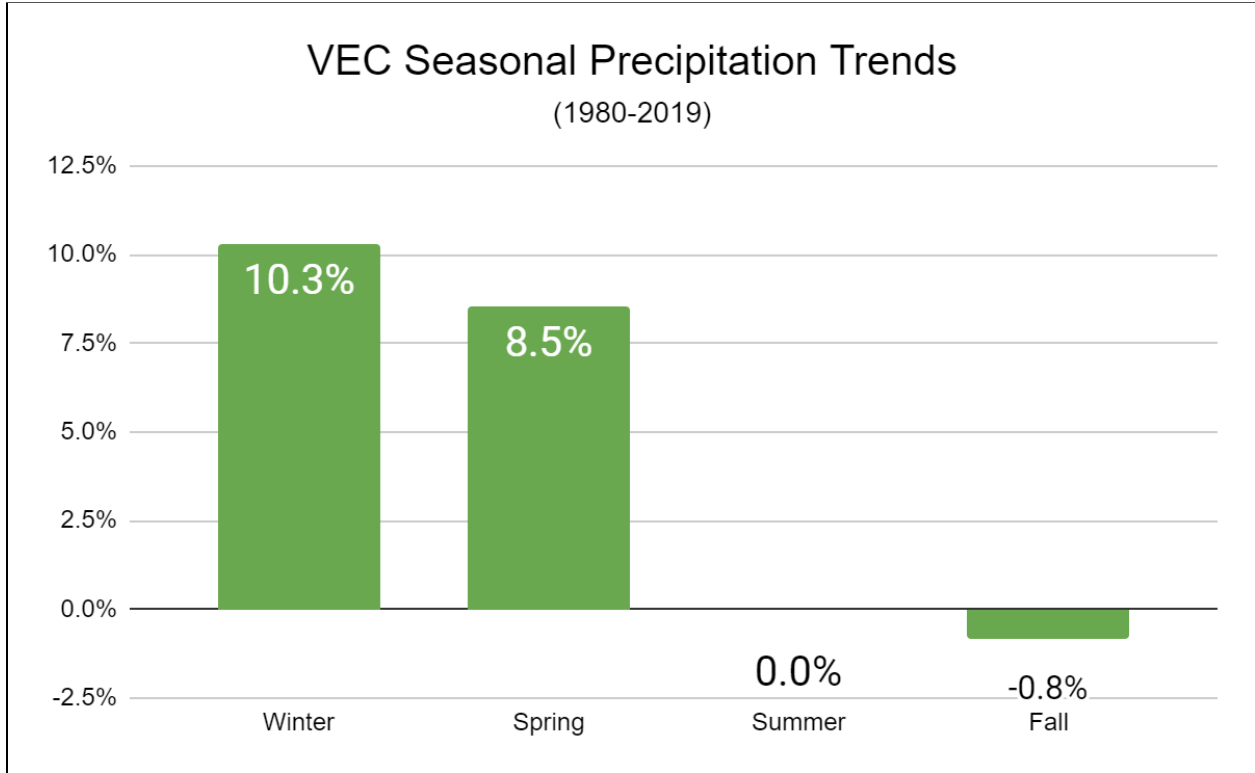


Figure 12. VEC region precipitation trend using the ERA5 30km reanalysis.

iii) Extreme Precipitation Climatology

Southern Vermont and the higher elevations saw the most extreme precipitation (Figure 13). These areas see 15 days or more of extreme precipitation (1" or greater in 24 hours). The rest of the state generally experienced 10 days or fewer of extreme precipitation (the majority of these events are rainfall). The higher amounts in southern Vermont are consistent with other work showing greater proximity to coastal storm systems (Perica et al, 2015). Higher precipitation occurrence in higher elevations is due to a combination of terrain-induced processes and limitations from model downscaling.

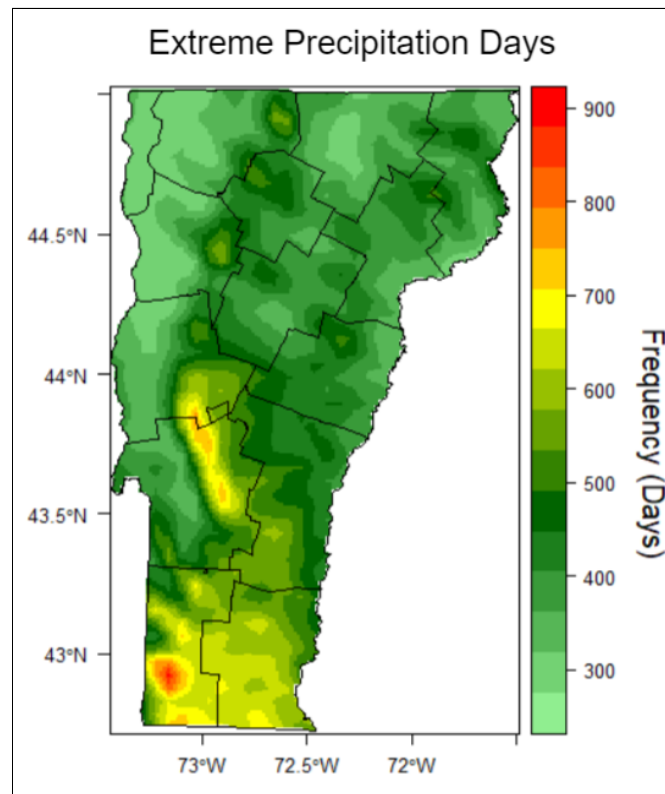


Figure 13. Frequency where precipitation was greater than 1 inch in a 24 hour duration from 1980-2019 using the downscaled ERA5 5km dataset.

iv) Extreme Precipitation Climatology Trends

The majority of Vermont saw increases in extreme precipitation events from 1980-1999 to 2000-2019. General increases were approximately 2 to 3 days a season from 1980 to 2019, with Caledonia and Essex counties showing greatest increases (Figure 14). Extreme precipitation days were less frequent over the northern portions of Lake Champlain and across Franklin county. This overall increase pattern is consistent with coastal storm systems and their widespread precipitation influencing greater extreme precipitation in eastern and southern Vermont.

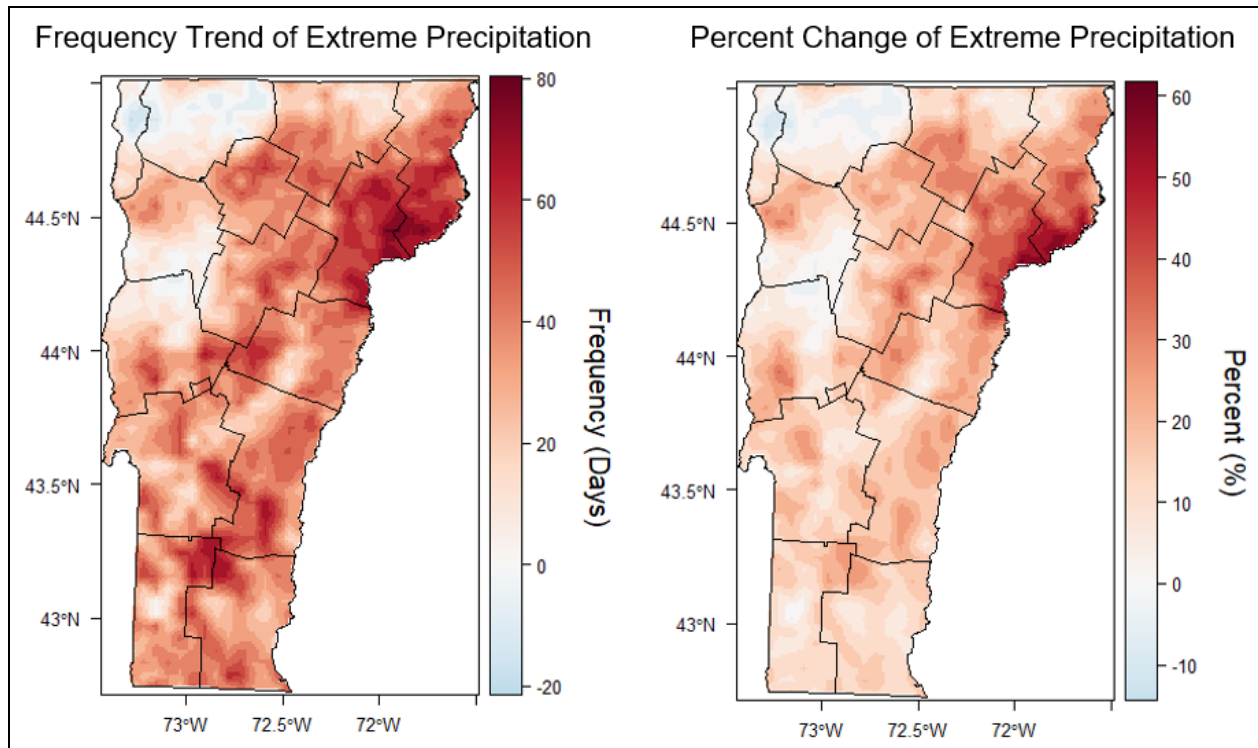


Figure 14. Difference in extreme precipitation days (days with precipitation greater than 1 inch) between 1980-1999 and 2000-2019 (left). Percent change in extreme precipitation days (days with precipitation greater than 1 inch) between 1980-1999 and 2000-2019 (right). Data source is the downscaled ERA5 5km.

v) Precipitation Phase

The majority of Vermont's precipitation reaches the ground as unfrozen hydrometeors with 78% of the total precipitation being rainfall. Snowfall accounts for around 21% and freezing rain is around 1%. (Figure 15). Freezing rain estimates are likely on the high side based on the FRAM ice accretion model used (Sanders and Barjenbruch 2016). There was no substantial change in the distribution of precipitation from 1980-2019 in rain vs. snow, however the 2010s did feature the highest amount of freezing rain precipitation. Warmer and wetter winter storm systems are more likely to have conflicts with air temperatures around freezing, likely producing more mixed-phase storm systems.

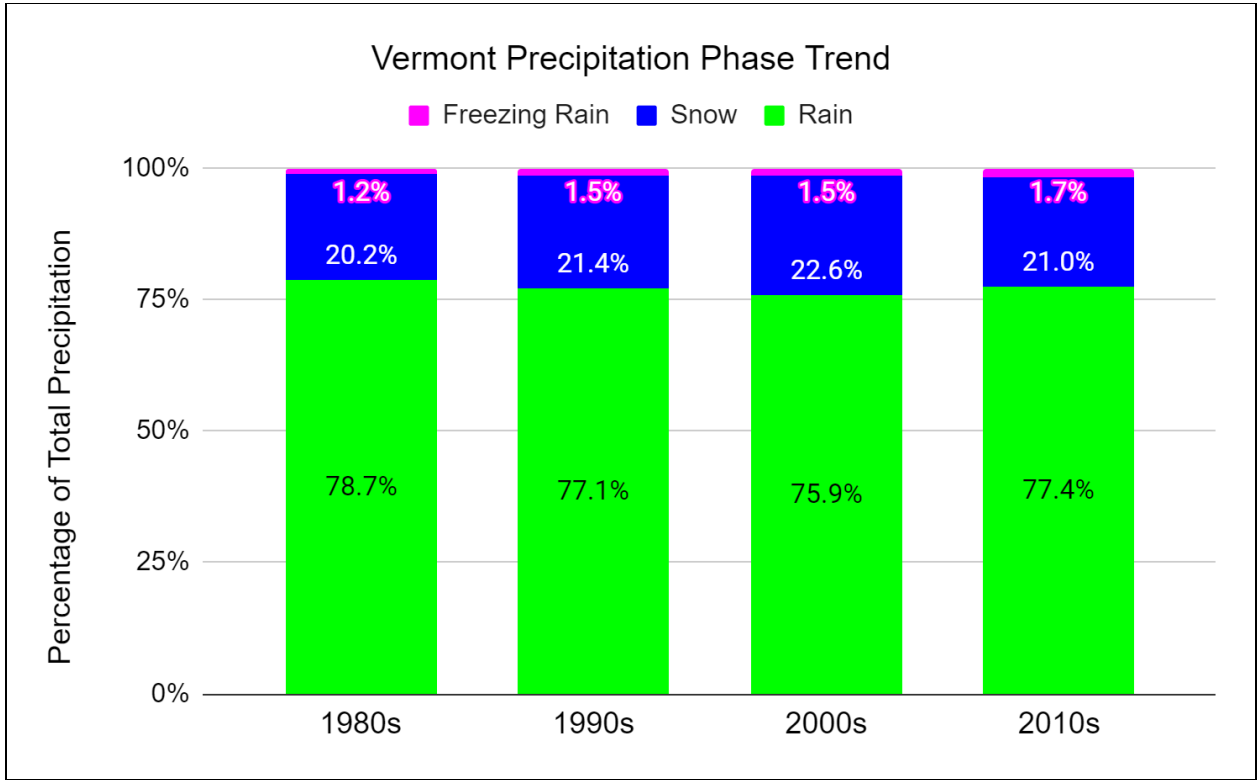


Figure 15. Percentage of precipitation amount by type for Vermont for each decade from 1980-2019. Data source is ERA5 30km.

4) Hazard Climatology

A variety of weather hazards may cause damage to the electric power system. This work focuses on large-scale or gradient winds, wet snow icing, and freezing rain icing. The climatology of these hazards is provided in more detail to understand locations generally at greater risks.

a) Gradient Wind Climatology

Gradient wind systems are typically associated with large-scale midlatitude storm systems. These storm systems have two general classes, those that track to the north of Vermont with strong backside westerly to northwesterly winds, and those that track to the east of Vermont that often come from the south with a more coastal track origin. The latter storm systems are often associated with a tropical storm system or hurricane interacting with a midlatitude storm system (e.g., Tropical Storm Philippe - October 2017). Topography plays an important role influencing the location of high winds, with winds generally increasing with elevation (Figure 16). The windiest lowland locations include the Champlain Valley and near Lake Champlain where pressure-gradient channeling often occurs with north to south flow.

There is a high sensitivity of peak winds to wind direction. Topography plays an important role with the orientation of terrain to wind direction where terrain may enhance or suppress wind speeds. Higher elevations generally experience a higher frequency of strong winds as wind speeds typically increase with height. Wind speed enhancement may occur from downsloping wind storms where the flow breaks as a wave on the lee side of barriers causing higher winds in lower elevations away from terrain, or wind speed enhancement may occur due to terrain acting to mix winds aloft closer to leeside valleys. Terrain wind enhancement depends on a variety of complex factors such as atmospheric stability and the location and strength of the low-level jet. Northerly or southerly wind directions tend to have the highest frequencies in the Champlain Valley (Figure 17). Westerly winds, on the other hand, tend to be the most frequent and strongest in the southern Green Mountains and locations to the east (Figures 17 & 18). Southeasterly to easterly wind directions tend to be more likely east of the Green Mountains ranges.

The seasonal frequency of high winds shows that the greatest number of high wind days occurs in January while August has the lowest (Figure 19). Higher winds are more likely during the cold season when transient weather systems are stronger due to increased temperature gradients producing larger pressure gradient forces.

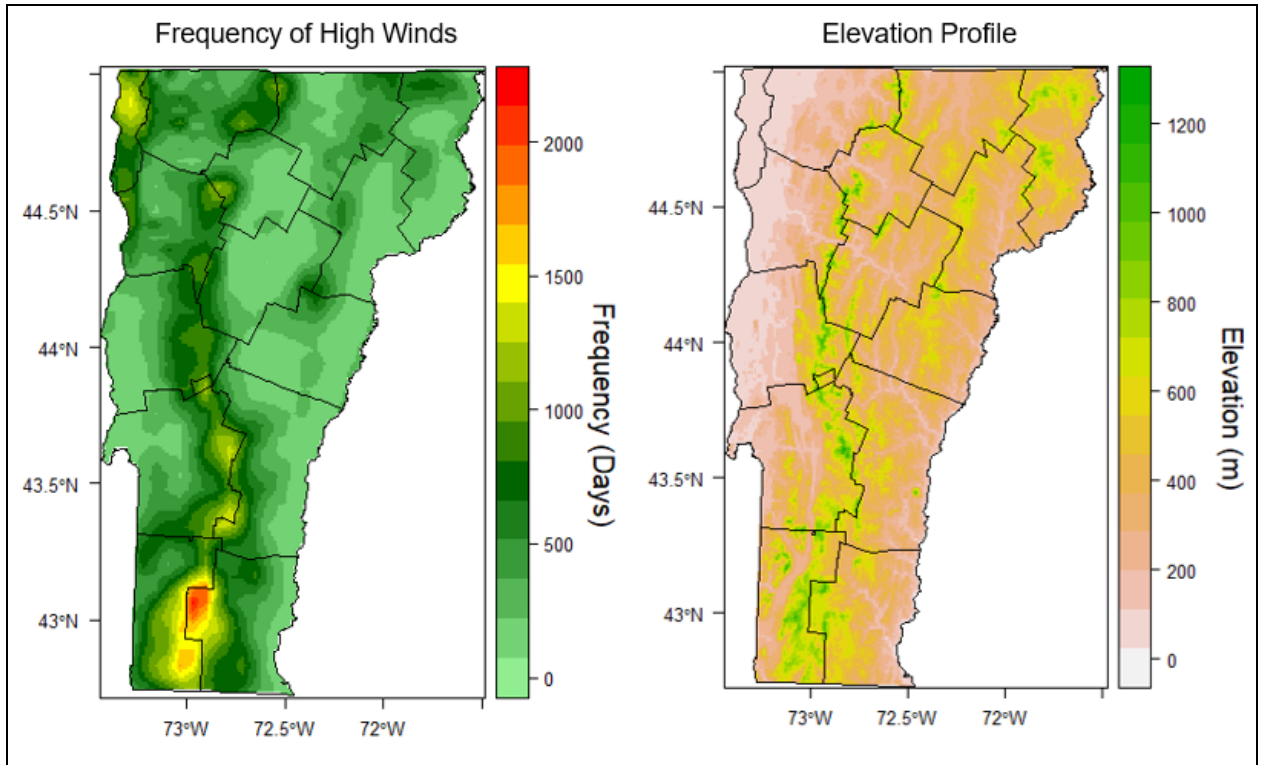


Figure 16. Days with 10-meter elevation wind gusts above 45 mph 1980-2019 (left) and elevation (right). Wind data source is the downscaled 5-km ERA5.

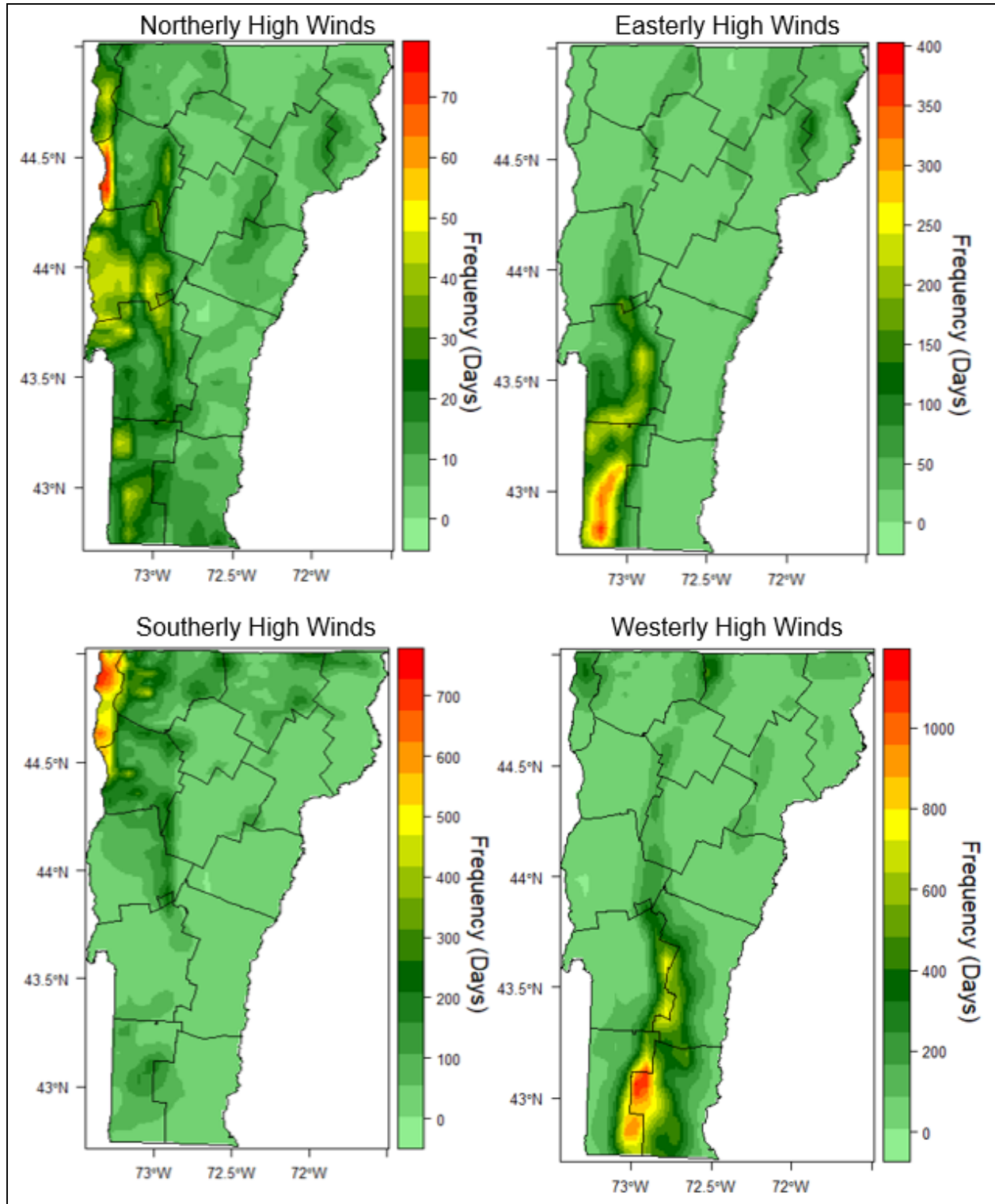


Figure 17. Frequency of high wind days by wind direction from 1980-2019 using the downscaled ERA5 5km dataset. A high wind day is defined as a day with a 10-meter wind gusts above 45 mph.

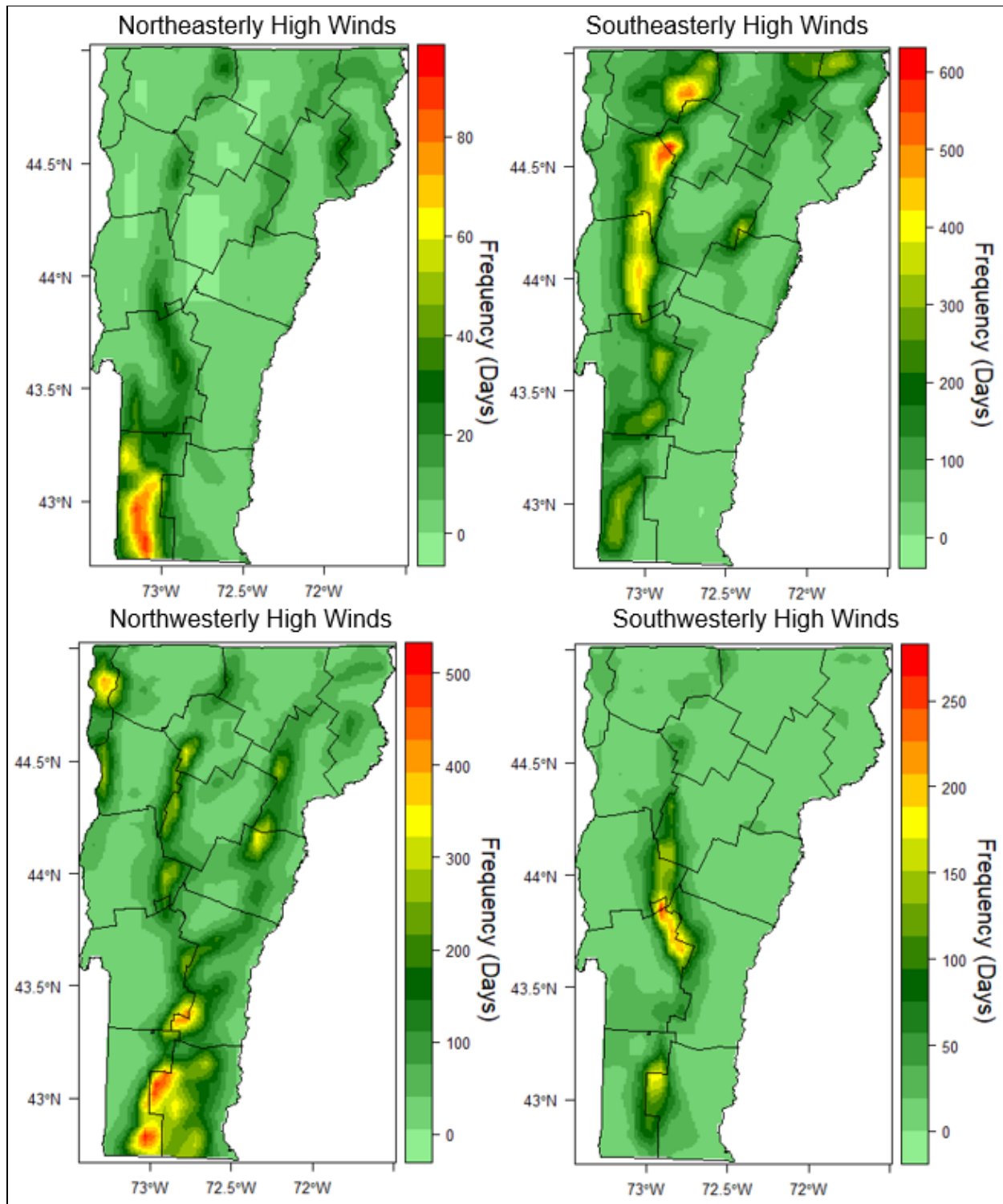


Figure 18. Frequency of high wind days by wind direction from 1980-2019 using the downscaled ERA5 5km dataset. High wind day is defined as a day with a 10-meter wind gusts above 45 mph.

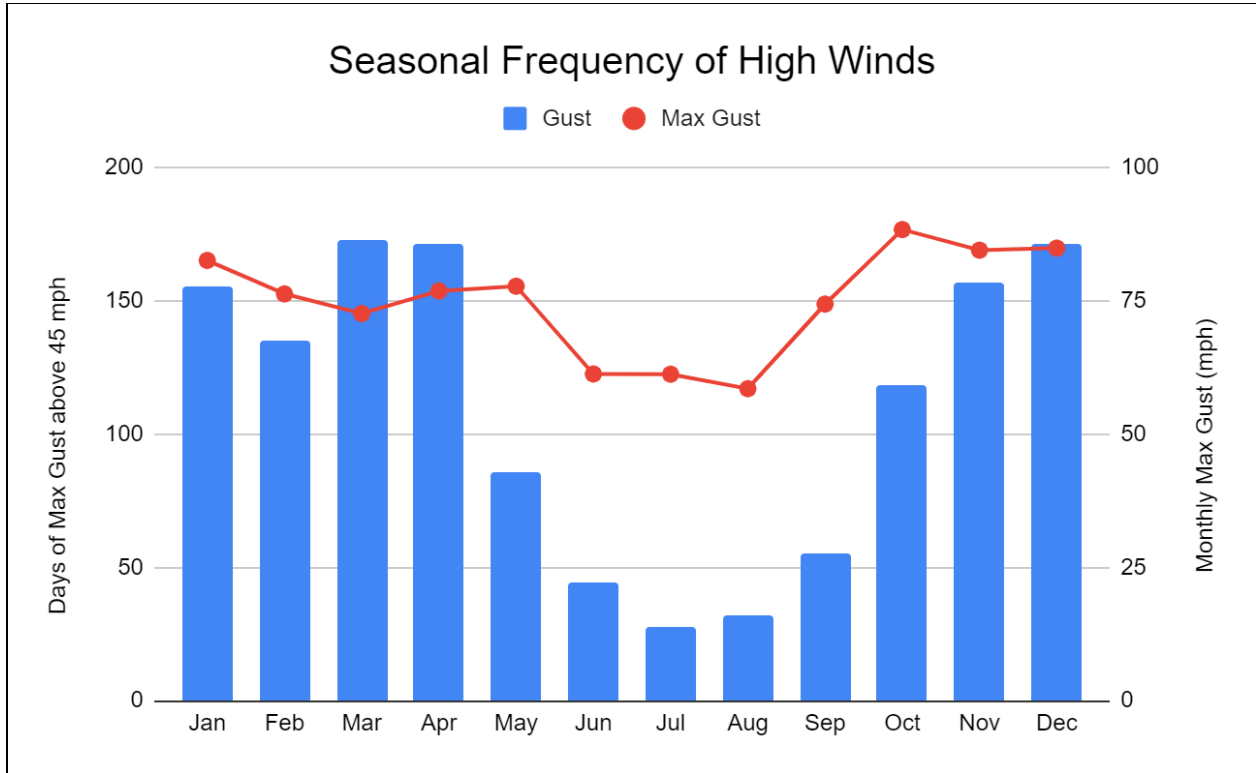


Figure 19. Days with Vermont spatial max gust at 10-m greater than 45mph aggregated monthly and spatial max monthly top gusts from 1980-2019 using the downscaled ERA5 5km dataset.

b) Gradient Winds Trends

The 20-year trend in gradient wind shows some spatial variability with high wind days declining slightly in the Connecticut River Valley within the Champlain Valley had a slight increase (Figure 20). Higher winds east of the southern Green Mountains in Windham county were likely associated with a higher frequency of westerly to northwesterly wind events, based on the climatology described in Figures 17 and 18. The general pattern suggests that locations with greater high wind event days had a higher frequency of windy days while locations with lower high wind frequency saw fewer from 1980 to 2019. The overall statewide aggregated change in gradient wind events featured negligible change from 1980 to 2019.

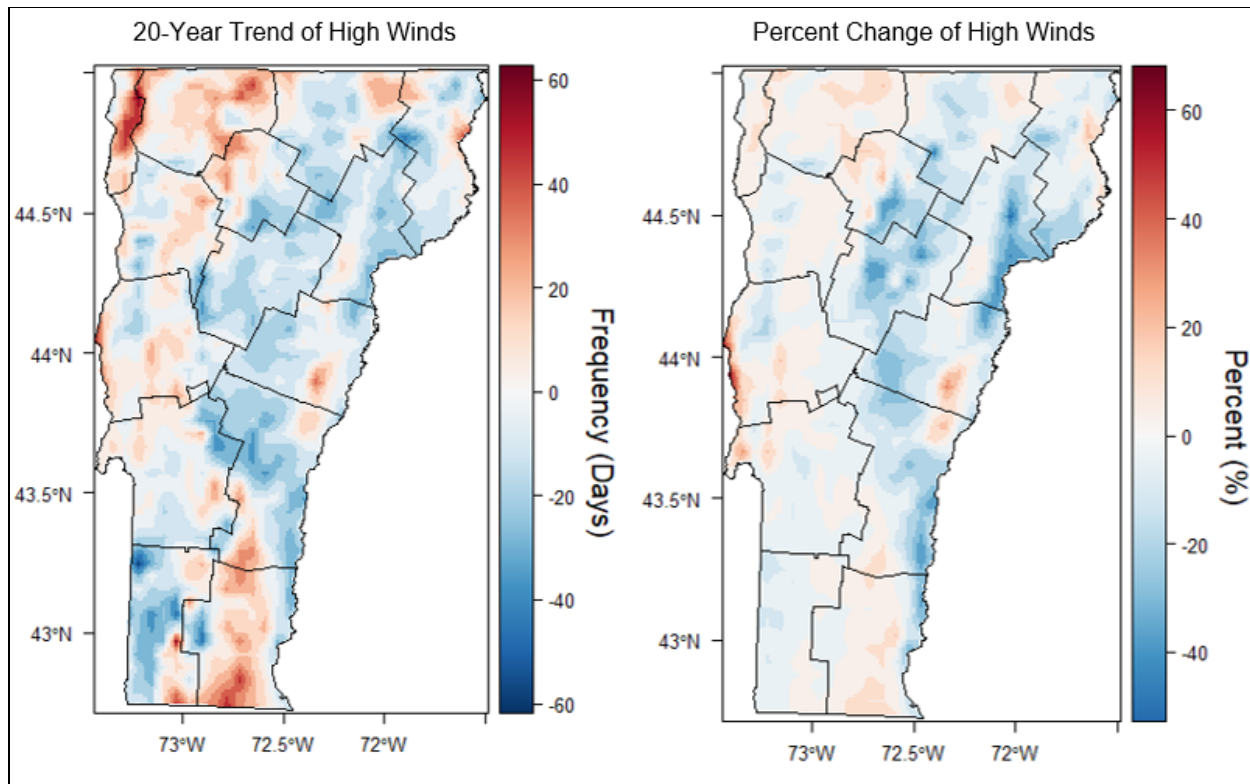


Figure 20. Difference in the number of extreme wind days between 1980-1999 and 2000-2019 using the downscaled ERA5 5km (left). Percent difference in the number of extreme wind days (right).

c) Wet Snow Icing Climatology and Trends

Wet snow icing occurs when partially melted snow flakes accrete or stick onto trees and/or powerlines. The weight of the wet snowfall often produces power outages by damaging trees within or near right of ways. Wet snowfall is defined when the reanalysis precipitation type was snowfall and the surface wet bulb temperature was greater than -2°C . The spatial climatology illustrates fairly wide varying accumulations, generally from less than 1 day to 2 days per year. A moderately strong elevation signal is identified, with lower elevations west of the Green Mountains featuring the fewest days, while areas east of the Green Mountain crest were more vulnerable (Figure 21).

The seasonal frequency of wet snowfall illustrates that all months during which snow can fall feature wet snowfall, with March and April having the highest peaks (Figure 22). Few mid-winter wet snowfall event days occurred as a result of colder temperatures producing a higher fraction of dry snowfall.

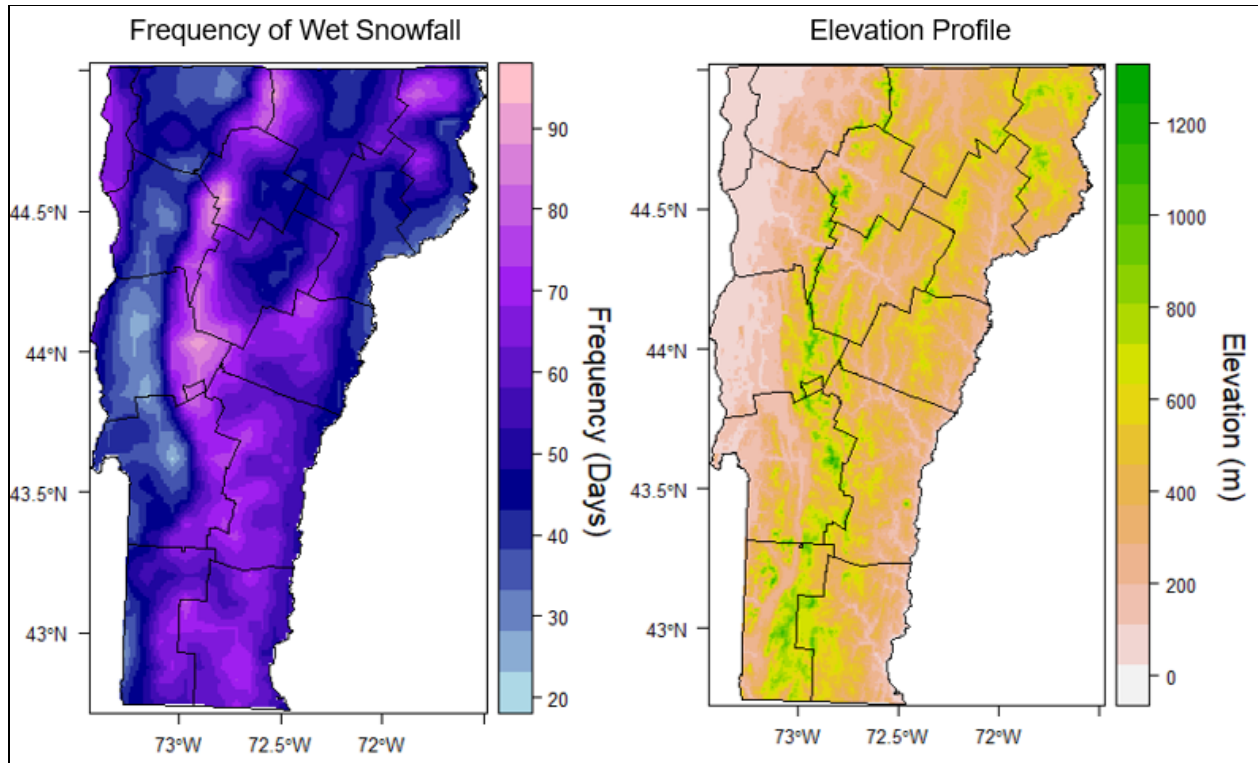


Figure 21. Total extreme wet snow days (wet snow liquid water equivalent is greater than 0.40" in a 24 hour accumulation period) for 1980-2019.

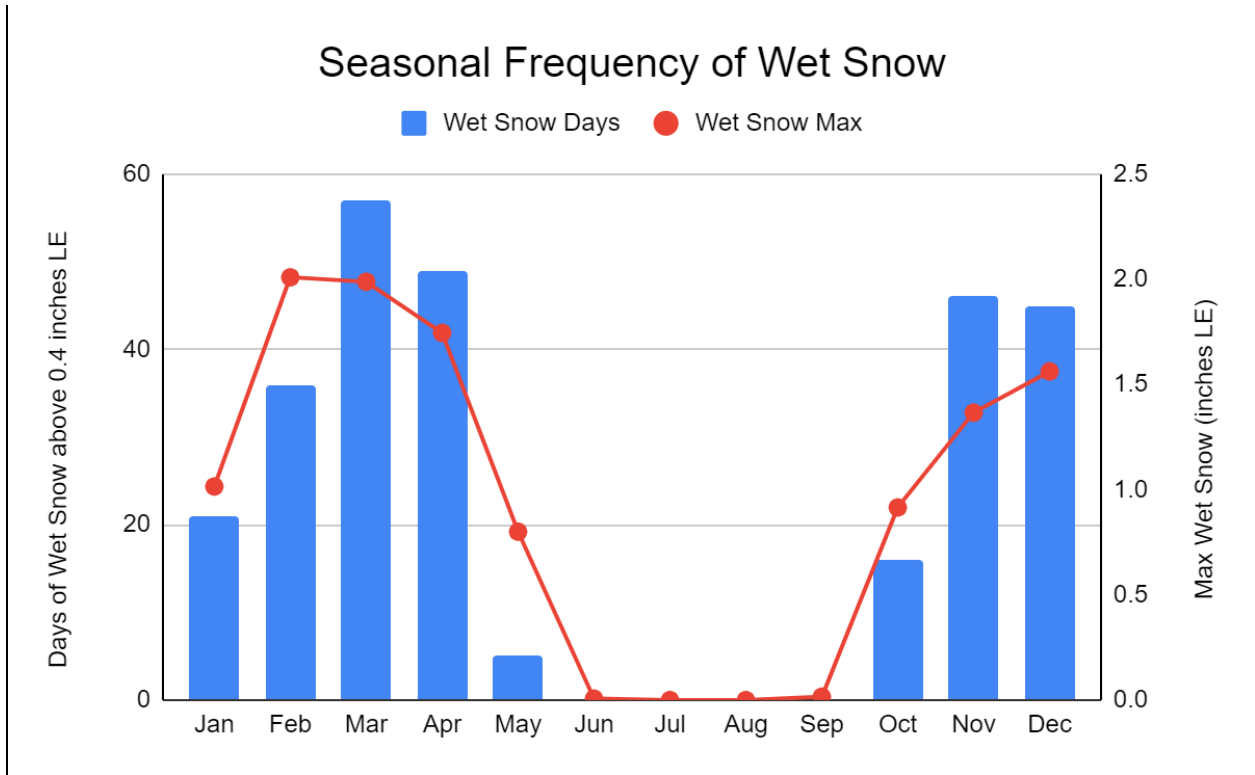


Figure 22. Vermont days of spatial max wet snow greater than 0.4” liquid equivalent (LE) aggregated monthly and monthly max wet snow using the ERA5 30km dataset. Accumulation duration was 24 hours.

With more mild winter temperatures and increased precipitation there was a general increase in the overall wet snowfall. This risk came primarily as more early-season snowfall events in late October through December (e.g., Dec 9-10, 2014). There was some spatial variability in wet snowfall trends with northeastern Vermont and southern Vermont seeing the greatest increases (not shown).

d) Freezing Rain Climatology and Trends

Freezing rain occurs when rain reaches the ground, vegetation, or infrastructure and freezes on contact (typically the air temperature is or has been recently below freezing). Freezing rain icing frequency is more prevalent in the higher terrain and Southern Vermont (Figure 23). Given the limitations of the ice accretion model and other challenges within determining precipitation phase in the downscaled model, the pattern of freezing rain likely underrepresents the frequency of freezing rain in some valley locations, in particular across the northern Champlain Valley. The ice storm of January 1998 featured some of the highest ice accretions in northernmost Valley locations and middle-elevation zones (1500-2500’ elevation) north of Montpelier (Miller-Weeks et al. 1999). In the nine years (2011-2019) of power outage analysis conducted within this work there was only one significant ice storm (Dec 21, 2013).

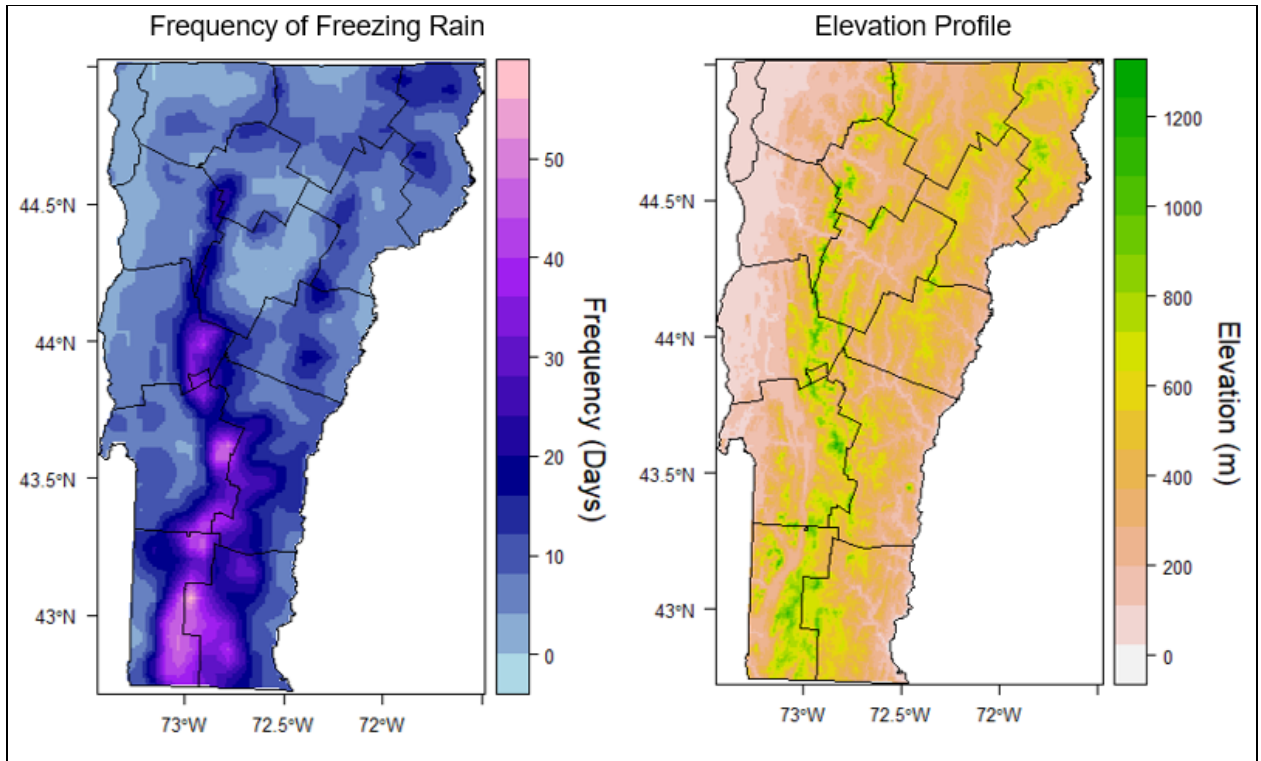


Figure 23. Total freezing rain days (ice thickness is greater than 0.25") for 1980-2019 using the ERA5 5km dataset.

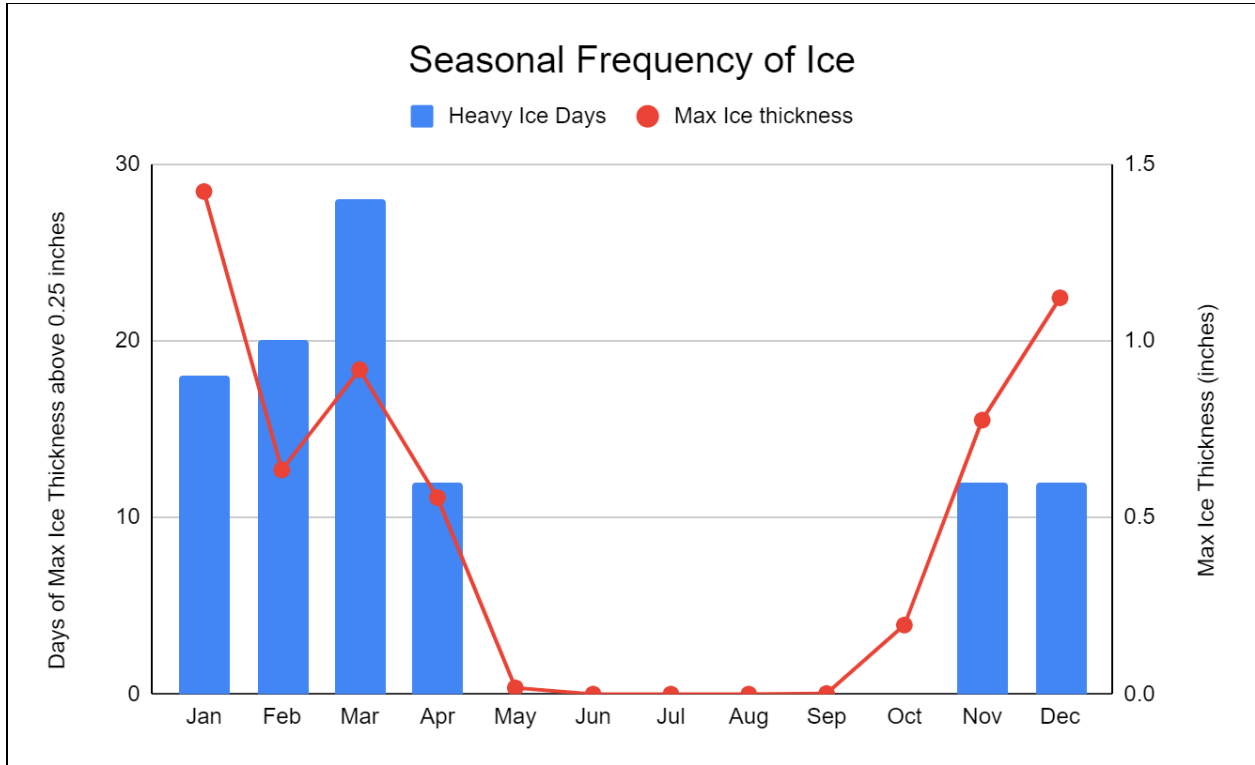


Figure 24. Vermont days of spatial max ice thickness greater than 0.25” aggregated monthly and monthly max wet snow using the ERA5 30km dataset (1980-2019).

The frequency of freezing rain icing is greatest during mid to late winter, with a March peak. The peak ice thickness occurred during the January 8, 1998 ice storm (Figure 24). Given the relatively small number of freezing rain icing days, no trend was able to be determined. However, an increase in the number of low-end freezing rain days was observed for ice accumulations of 0.10” and above; this is likely related to more mixed-phase storm systems.

5. Outage Analysis

a. Hazard Climatology

Extreme weather events feature significant seasonal variability with the cold season bringing the highest number of high-wind events, and late summer to early fall featuring the greatest risks for widespread heavy rainfall (Figure 25). As a fraction of overall risk, wind represents the greatest overall hazard; this is primarily through gradient or large-scale wind events. Heavy rainfall has a peak occurrence during October when tropical moisture related to remnant or active tropical storm systems may interact with midlatitude storm systems to produce widespread or organized precipitation. It should be noted that this work did not conduct hydrologic modeling or other flood impact analysis to determine the degree to which heavy rainfall may have produced any electric grid impacts. Flooding is a comparatively low risk to other hazards described in Figure 25, although potentially high-impact when major storm systems are involved (e.g., Tropical Storm Irene, Anderson et al 2017). Heavy rainfall combined with high wind events do often aggravate the risk for outages, when soil moisture content is high and may contribute to the risk of trees uprooting.

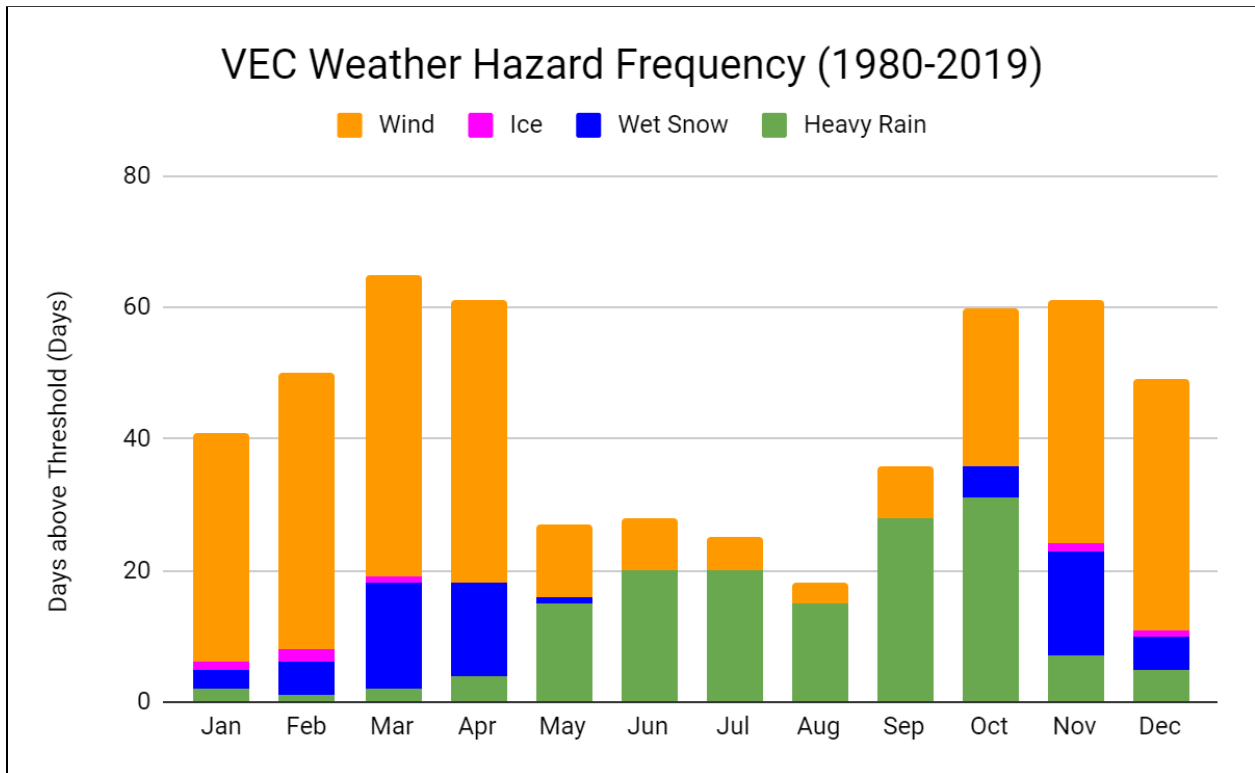


Figure 25. Average days a year reaching above the following extreme weather thresholds as defined with the VEC polygon. Rainfall 1.0 inches or greater, wet snowfall - 0.4 inches liquid equivalent or greater, ice thickness - 0.25 inches or greater, spatially averaged wind gust - 45mph. Data source includes ERA5 30km for precipitation variables and the ERA5 5km dataset for wind.

b. Distribution System Outage Climatology

Power outage data was provided by VEC from 2011-2019. This data was aggregated daily and statewide from 2011-2019. The seasonal frequency shows two peaks, one in July and a fall and early winter peak (Figure 26). Fewer mid-winter outages are likely associated with seasonal system self-hardening from cold temperatures, trees after leaf drop, and more resilience after some fall weather events.

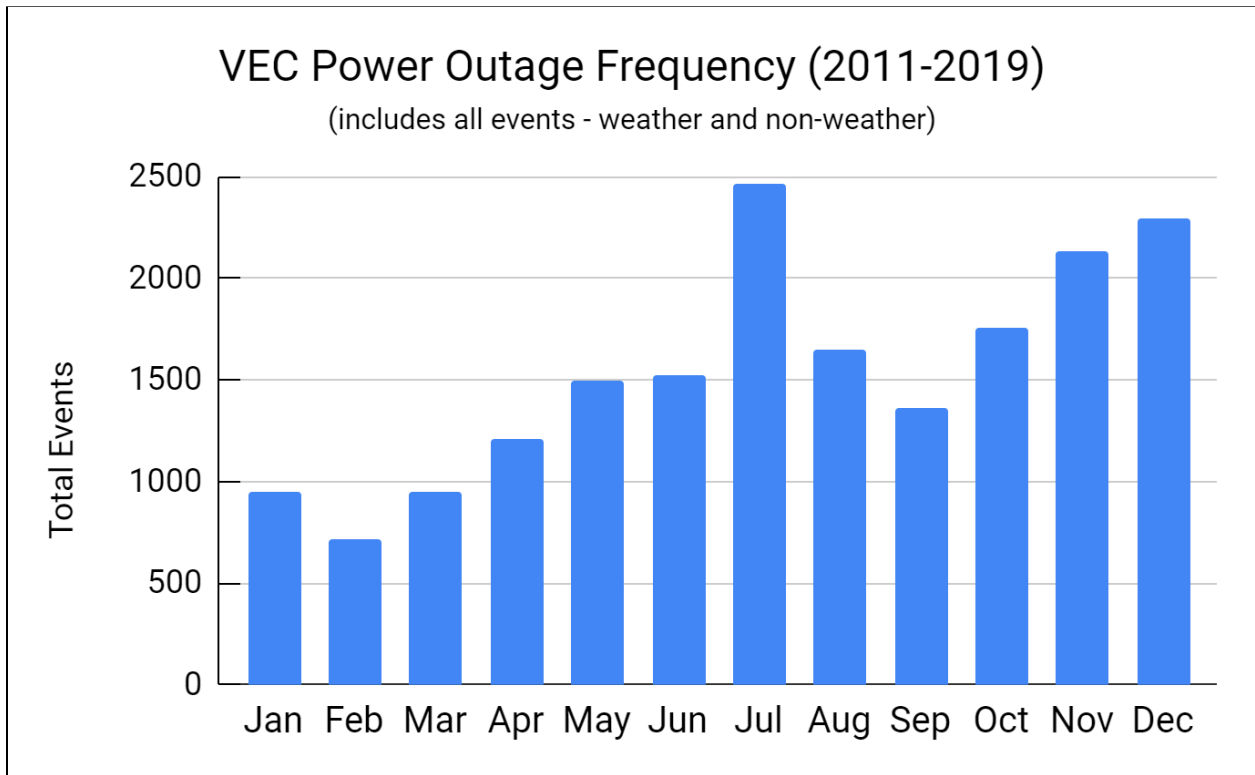


Figure 26. Total distribution system power outage events from 2011-2019 by month.

The frequency of power outage events and their weather attribution shows a thunderstorm peak during summer, likely as a result of localized wind gusts from thunderstorms, whereas wet snowfall impacts are concentrated in the fall to early winter (Figure 27). Gradient wind event impacts were also highest in the late fall and early winter (November and December).

The severity of power outage impacts can be represented by the duration of power outages; in this analysis customer power outage hours are described in Figure 28. The fall and early winter season featured over 50% of all power outage severity impacts from a combination of wet snowfall and high wind storms. January and February featured a comparatively low impact compared to the higher frequency of weather hazards (Figure 25). This strong seasonal signal should be incorporated into planning and emergency preparedness to take storm systems during the fall and early winter with a higher level of potential risk.

Wind events (gradient wind or thunderstorm) accounted for 60% of all distribution power outage impacts, whereas wet snowfall was 27% and ice was 13% (Figure 29). The differences

in the frequency and impacts of weather hazards was most dramatic for wet snowfall and thunderstorms. Thunderstorms generally featured a much lower impact while wet snowfall events featured a comparatively higher impact.

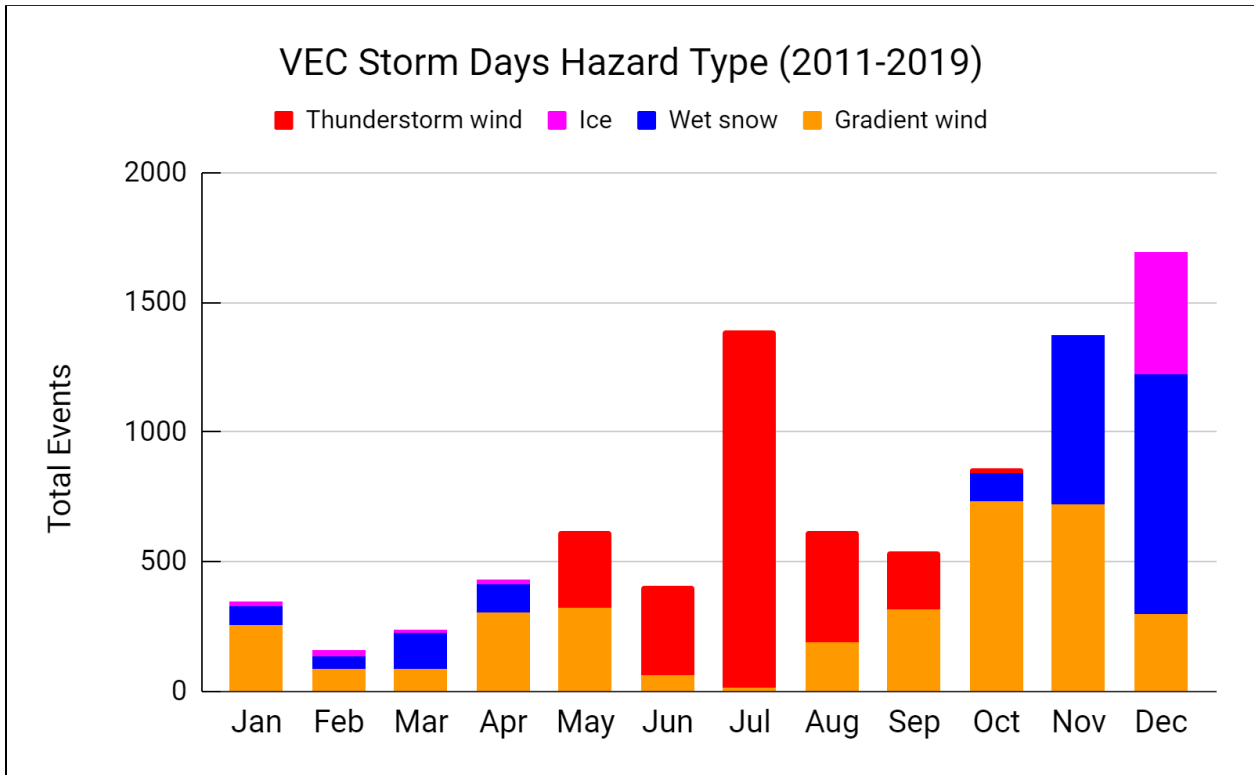


Figure 27.VEC storm days aggregated monthly according to type using total events.

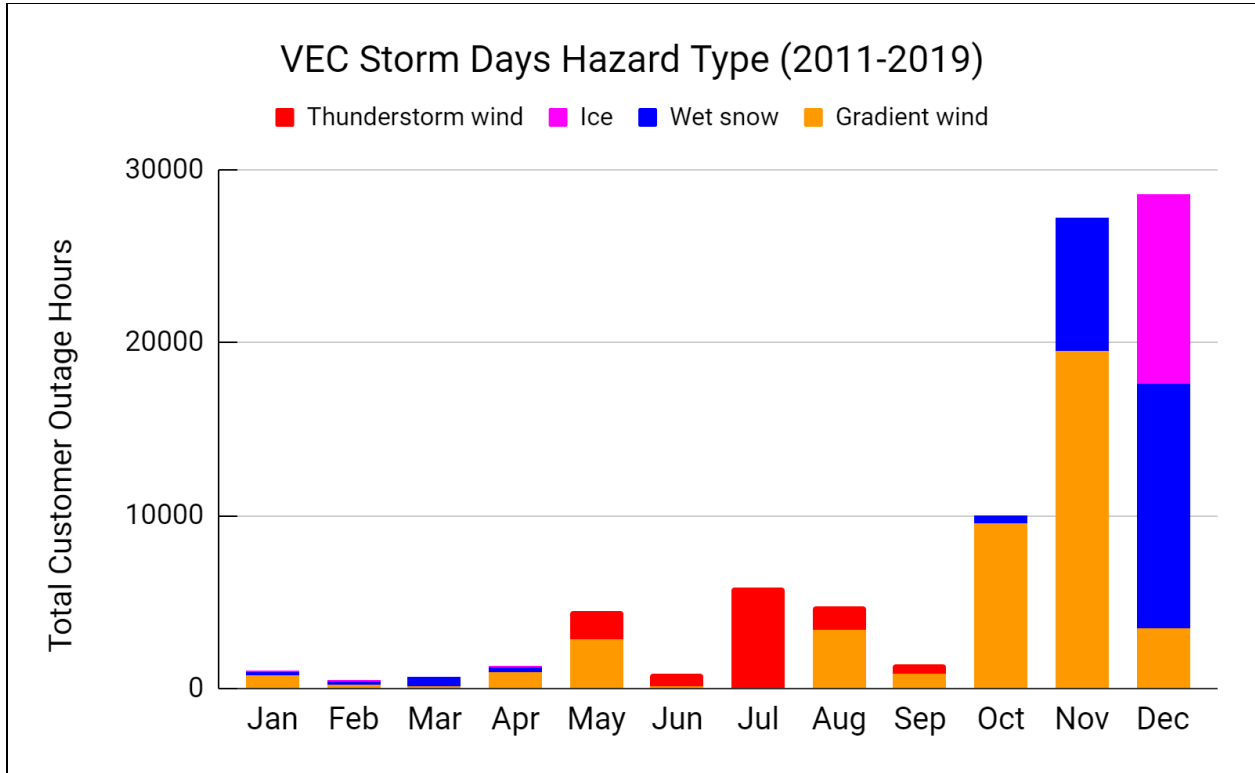


Figure 28. VEC storm days aggregated monthly according to type using customer outage hours.

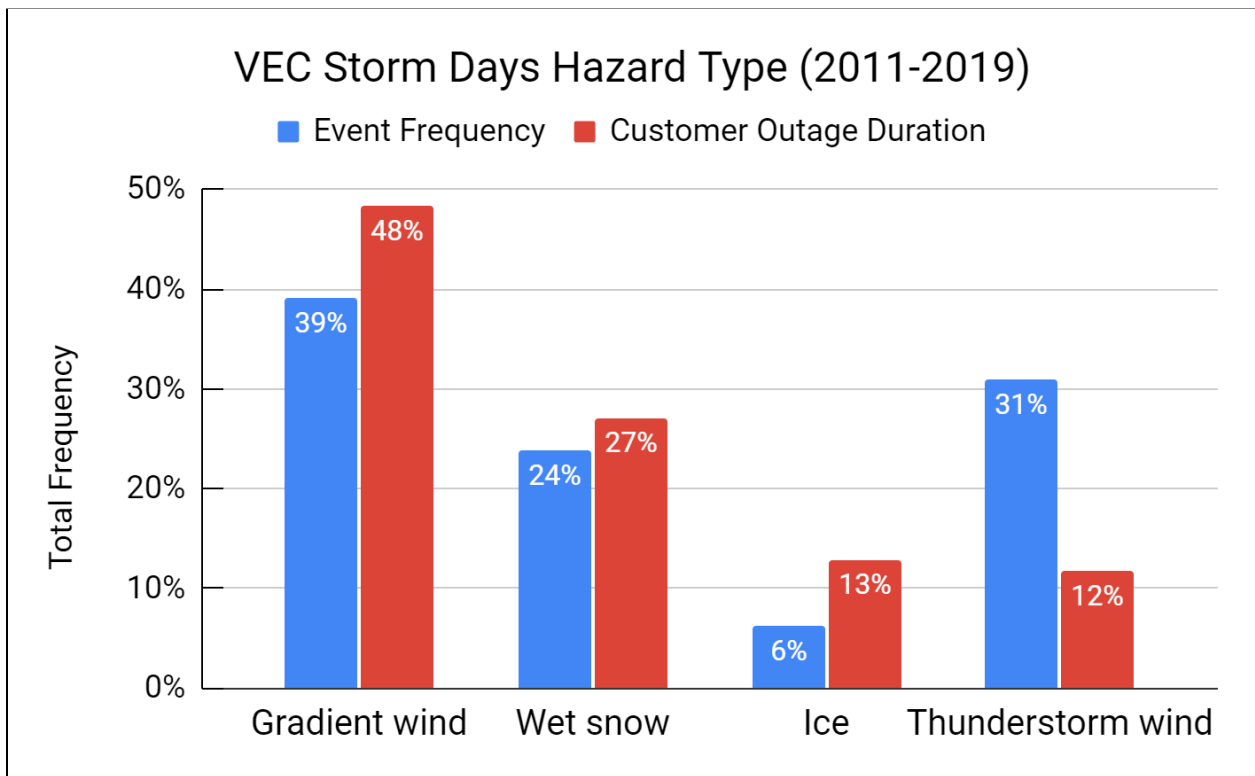


Figure 29. Event frequency percentage broken down according to hazard type.

c) Extreme Storm Examples

The top storms for each weather hazard and their respective customer outage profiles are described in Figure 30. The high wind storm of Oct 30, 2017 was the most significant storm, with nearly 23,000 members without power at the storm's peak and a 5-day restoration. The wet snow and ice events had a lower peak customer value, but more sustained outages as wet snow and ice remained loaded on trees and overhead lines, continuing to cause outages as restoration was underway. By comparison, the top thunderstorm event (July 23, 2012) peaked around 6,000 members without power with a full restoration in less than 2 days.

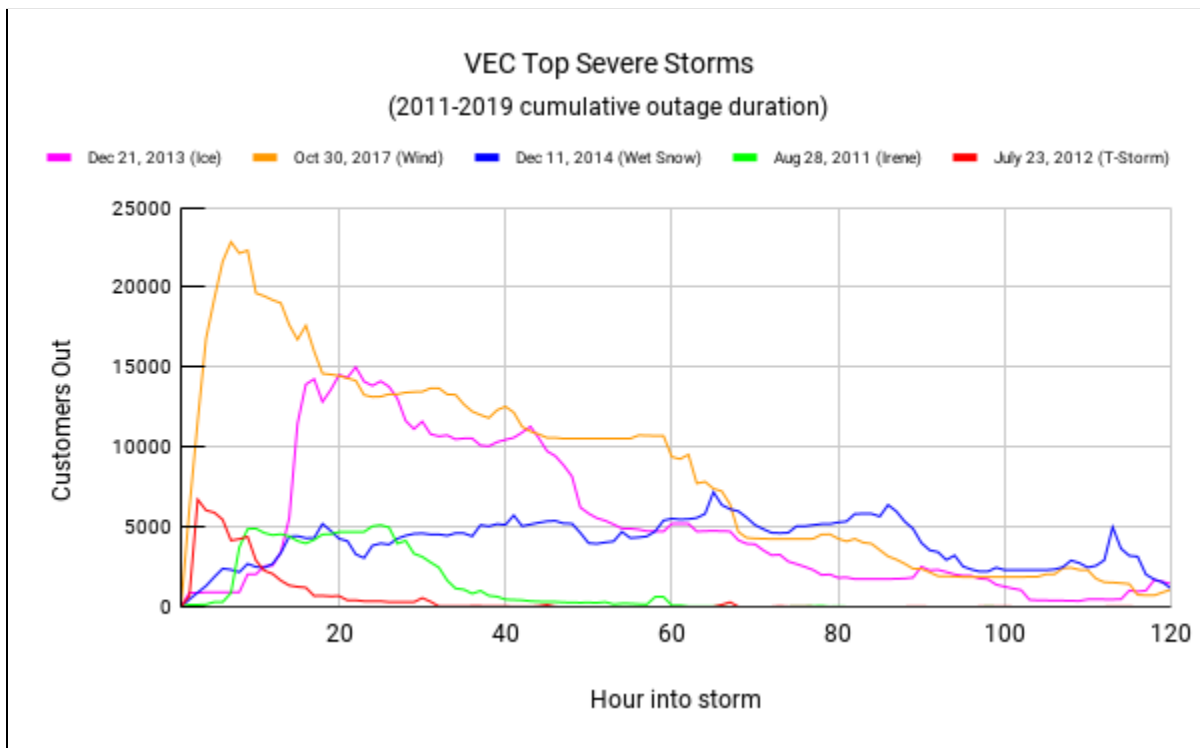


Figure 30. Top statewide power outage storm by storm class from 2011-2019.

d) Historic Power Outage Reconstruction and Trends

In order to describe long-term power outage variability a deep learning model was used to reconstruct or model outages outside of the observed outage window (2011-2019). Table 2 describes the variables used for the deep learning model. This reconstruction does not sample outages from thunderstorm events, and has a tendency to underestimate the most extreme storms; thus, the recreated values likely underestimate the total historic outages. This methodology also assumes stationarity with system infrastructure and doesn't take into account any system hardening over time. Nonetheless, this method can be used to understand general long-term weather impact variability.

The 2010s featured the highest number of simulated events (combining severe storm days and all days) (Figure 31), being the most active decade since 1980. The most severe

storms produced a higher fraction of overall impacts during the 2010s. In order to understand severe storm variability may be changing, this population is examined independently.

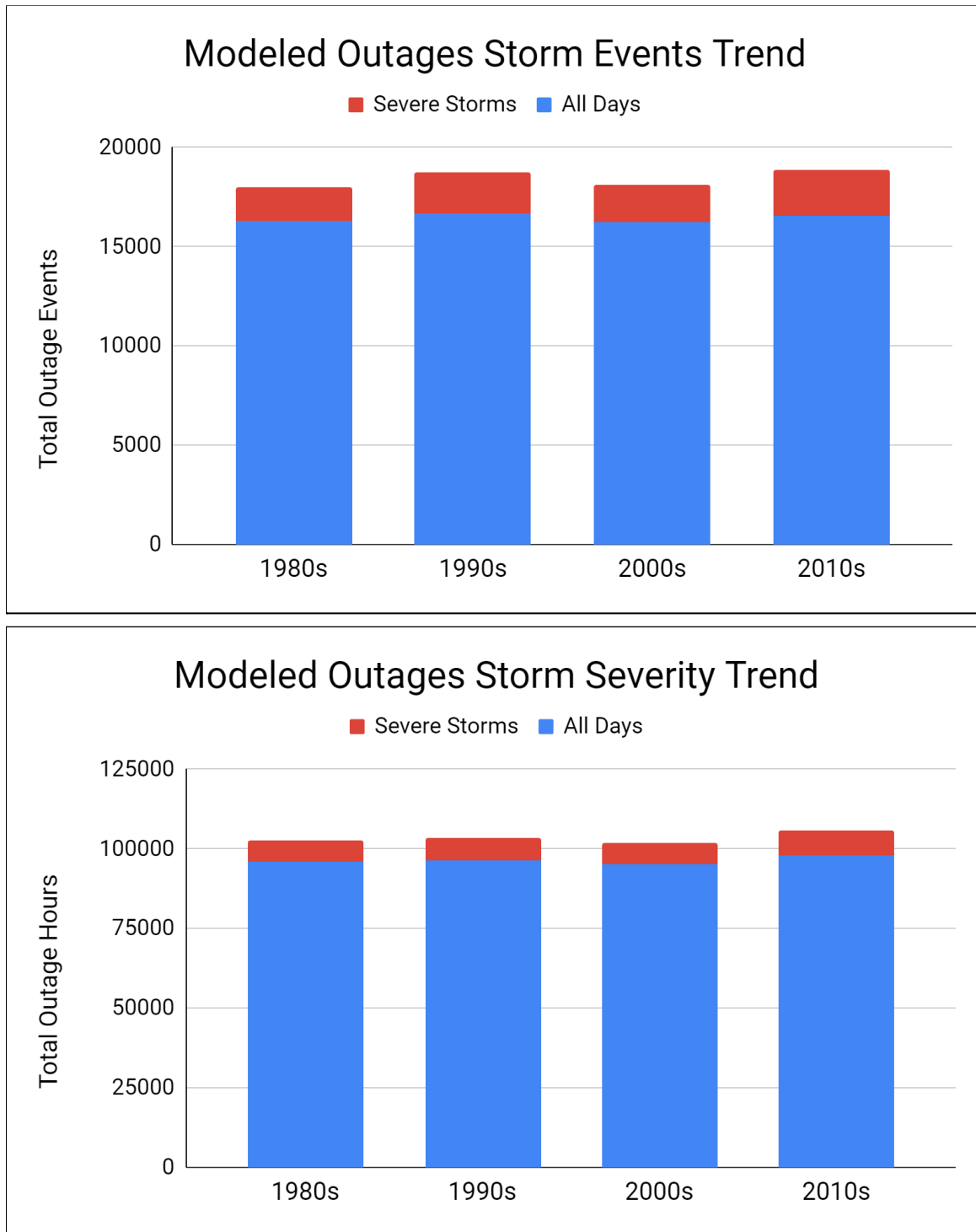


Figure 31. Historically modeled power outages using a deep learning model, top shows frequency variability while bottom describes the intensity variability. Severe storms are defined as being in the top 1% of storm days by total number of events.

e) Extreme Storm Analysis and Trends

In order to understand how the most extreme storms may be changing, the top most severe storms were subsetted. The top 1% of modeled storm days (defined around 30 daily events or greater) represented around 15% of all modeled impacts. Decadal variability of the most extreme storms shows that both the frequency and intensity of these storms has increased from 1980 to 2019 (Figure 32). Overall modeled storm frequency has decreased approximately -1% for all storms and showed no change for storm severity (Table 3). However, the most extreme storms increased frequency by 11% and were 7% more severe (Table 3). This result suggests that the most severe or extreme storms are getting more frequent and intense.

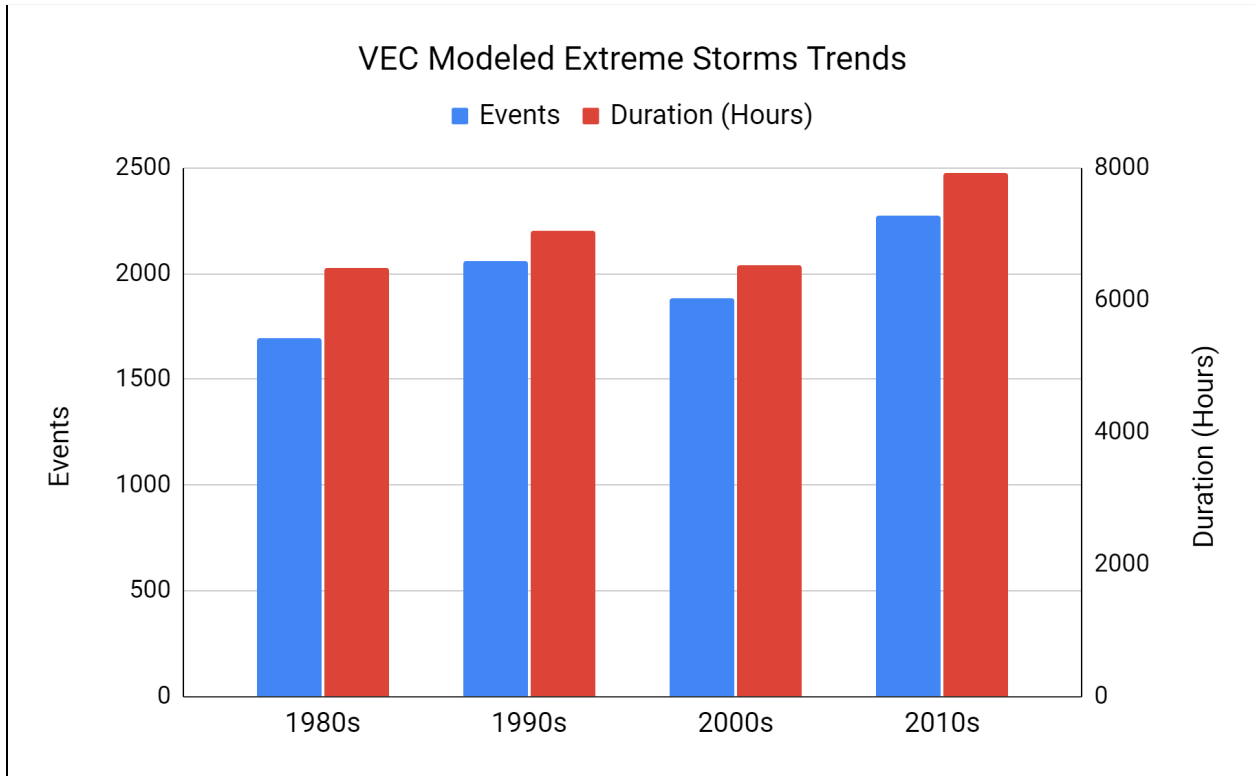


Figure 32. Most extreme reconstructed storm outage impacts by frequency (events) and severity (duration). Extreme storms represent the top 1% of overall events.

| Timeframe | All Modeled Days | | Extreme Modeled Storms | |
|----------------------|------------------|----------------|------------------------|----------------|
| | Total Events | Total Duration | Total Events | Total Duration |
| 1980-1999 | 32970 | 192667 | 3752 | 13531 |
| 2000-2019 | 32800 | 193159 | 4160 | 14437 |
| 20-Year Trend | -1% | 0% | 11% | 7% |

Table 3. Modeled power outage trends. Extreme storm days were defined as the top 1% of all modeled storm events.

6. Climate Projections

In order to determine the future climatic shifts and how the weather behavior may vary within changing climatic states a combination of three information sources are relied upon. These include the current trends, climate simulations, and published literature. The trends are generally relied upon more than the simulations, with the literature being fairly limited for understanding extreme weather behavior. A general direction and level of risk are described to capture future risk and any adaption or resilience decisions that may be based on this analysis.

a) Base Climate States

Two climate simulations were run using two different emissions scenarios, the RCP4.5, which is considered a moderate greenhouse gas emissions mitigation pathway, and RCP8.5, which is considered the business as usual pathway with little mitigation of greenhouse gas emissions. Both simulations show limited variability with each other regarding future climate measures of temperature, precipitation, and solar radiation (Table 4). The simulations generally show a notable projected increase in temperatures, but relatively small changes to annual precipitation and solar radiation. The projected temperature increase was distributed fairly uniformly across all seasons and there were no significant seasonal changes to precipitation and solar radiation (not shown).

| Variable | 1990-2019 Baseline | RCP4.5 Simulation | RCP8.5 Simulation |
|--|-----------------------|----------------------|----------------------|
| Average Annual Temperature (°F) | 38.2 | 40.2 | 40.3 |
| Average Annual Precipitation (Inches) | 52.8 | 53.4 | 53.1 |
| Average Daily Solar Radiation (Watts/m ²) | 3697 | 3664 | 3668 |

Table 4. Climate simulations and base states. Simulations were run from 2020-2049.

The official forecast from this analysis incorporates three primary information sources: the long-term trend from 1980-2019, the two dynamically downscaled climate simulations, and published literature. These three information sources are synthesized to produce a general direction and level of confidence of each weather hazard and climate state (Table 5). The two high confidence forecasts include increases to temperature and extreme precipitation events. Extreme precipitation events have been increasing about twice the rate of average annual precipitation. Climate simulations were unable to resolve extreme events, in particular wind storms; this is a known issue with simulating extreme midlatitude weather events. Annual temperatures and precipitation are projected to increase while there is no significant change for annual solar radiation.

| VEC Climate and Weather Forecast Changes: 1990-2019 to 2020-2049 | | | | | |
|--|--------------------|---------------------|----------------------|------------------------------------|------------------------------|
| Variable | 1980 to 2019 Trend | Climate Simulations | Literature Consensus | Official Forecast Direction Change | Official Forecast Confidence |
| Annual Temperature | ++ | +++ | ++ | ++ | High |
| Annual Precipitation | + | 0 | + | + | Medium |
| Annual Solar Radiation | 0 | 0 | 0 | 0 | High |
| Wind Storms | + | - | + | + | Medium |
| Wet Snow Storms | + | 0 | NA | + | Medium |
| Ice Storms | + | + | 0 | 0 | Low |
| Heavy Precipitation Events | ++ | 0 | ++ | ++ | High |

| Sign Change Key | | Annual Temperature | Annual Precipitation | Wind Storms | Wet Snow Storms | Ice Storms | Heavy Precipitation Events |
|-----------------|---------------------|--------------------|----------------------|-------------|-----------------|-------------|----------------------------|
| +++ | Strong increase | +2 to +3°F | +5 to 7" | | | +11 to 15% | |
| ++ | Moderate increase | +1 to +2°F | +3 to 5" | | | +6 to 10% | |
| + | Slight increase | +0.3 to 1°F | +1 to 2" | | | +2 to 5% | |
| 0 | Little to no change | -0.2 to +0.2°F | -1 to +1" | | | -2 to +2% | |
| - | Slight decrease | -0.3 to -1°F | -1 to 2" | | | -2 to -5% | |
| -- | Moderate decrease | -1 to -2°F | -3 to 5" | | | -6 to -10% | |
| --- | Strong decrease | -2 to -3°F | -5 to 7" | | | -11 to -15% | |

Table 5. Official forecasts and sign changes for each predicted variable with accompanying forecast confidence.

b) Extreme weather events

Extreme weather events were examined in three major categories with respect to future projections. Hazards from thunderstorms (wind gusts and flash flooding) were not examined extensively, as there is limited literature in these areas and the scientific certainty is low given the complexities around convective processes. All three major large-scale storm classes (wind, wet snow, and ice) have distribution system outages that are anticipated to increase through 2049 (Table 6). The general fraction of outage risks is not projected to change significantly from historic values, with wind storms remaining the most significant threat to distribution system outages.

Increases in storm risk arise more from storms becoming more intense than frequent. A warming climate does generally provide more capacity for wind storms such as those related to tropical storms/hurricanes interacting with mid latitude storm systems to be more intense. A warming atmosphere also produces a greater potential for heavy precipitation events (Table 5). The low frequency of ice storms combined with the phase challenges makes ice storms a low confidence forecast. Overall distribution system power outages are projected to increase approximately 6% through 2049 compared to the prior thirty years with a moderate level of confidence.

| VEC Power Outage Risk Profile Projection: 2020 to 2049 | | | | | | |
|--|-------------------------|------------------|------------------|-----------------------|--------------|-----------------------|
| Hazard | Fraction of Outage Risk | Frequency Change | Intensity Change | Projection Confidence | Overall Risk | Overall Risk Change % |
| Wind Storms | 55% | 0 | + | Medium | +++ | +3 to +5% |
| Wet Snow Storms | 32% | + | + | Medium | ++ | +8 to +12% |
| Ice Storms | 13% | + | 0 | Low | + | 0 to +2% |
| Overall Risk Change | | | | | | +5 to +7% |

Table 6. Distribution system power outage risk assessment projection. Does not include winds from thunderstorms.

The climate simulations generally show a higher number of wet snow and freezing rain ice events during the winter season (Figure 33), which is consistent with a warming climate producing more storms that cross precipitation type/phase as a result of varying temperatures throughout storm systems. These factors suggest that the winter storm season will feature greater outage impacts. Both climate simulations show similar behavior to the frequency of wet snow and ice events; these results also support the idea that the climate will still remain cold enough across northern Vermont to sustain and increase wet snow and ice risks. However, as the climate warms there will be a tipping point sometime after these climate simulations end in 2049 where more rainfall dominates winter precipitation, reducing the frequency of snow and ice.

Figure 34 examines weather hazards and climate changes and their general sign changes and levels of confidence. High confidence changes occur with temperature, with extreme heat being more likely. For precipitation, extreme precipitation events, which are usually heavy rainfall, are increasing faster than annual precipitation with a fairly high degree of confidence. Low confidence forecast weather behavior includes ice storms and thunderstorms. The occurrence of drought is also likely to increase, despite increases in precipitation, thus the variability of precipitation both year to year and within seasons is likely to increase.

Influences on vegetation health and growth primarily arise from temperature and precipitation variability. The growing season is generally projected to increase, however, year-to-year precipitation variability and a variety of other factors (e.g., invasive species, species migration) make this work difficult to determine how vegetation management may be impacted. The climate generally appears fairly stable for vegetation health and growth through 2049, thus no substantial impacts on vegetation are able to be determined within this work. The asynchronous nature of tree growth responding to environmental stimuli and limited tree data sets prohibited more comprehensive results with how climate change may affect vegetation management. Figure 34 generally shows that most weather and climate risks are changing in a direction that increases overall risks to the distribution and transmission grid.

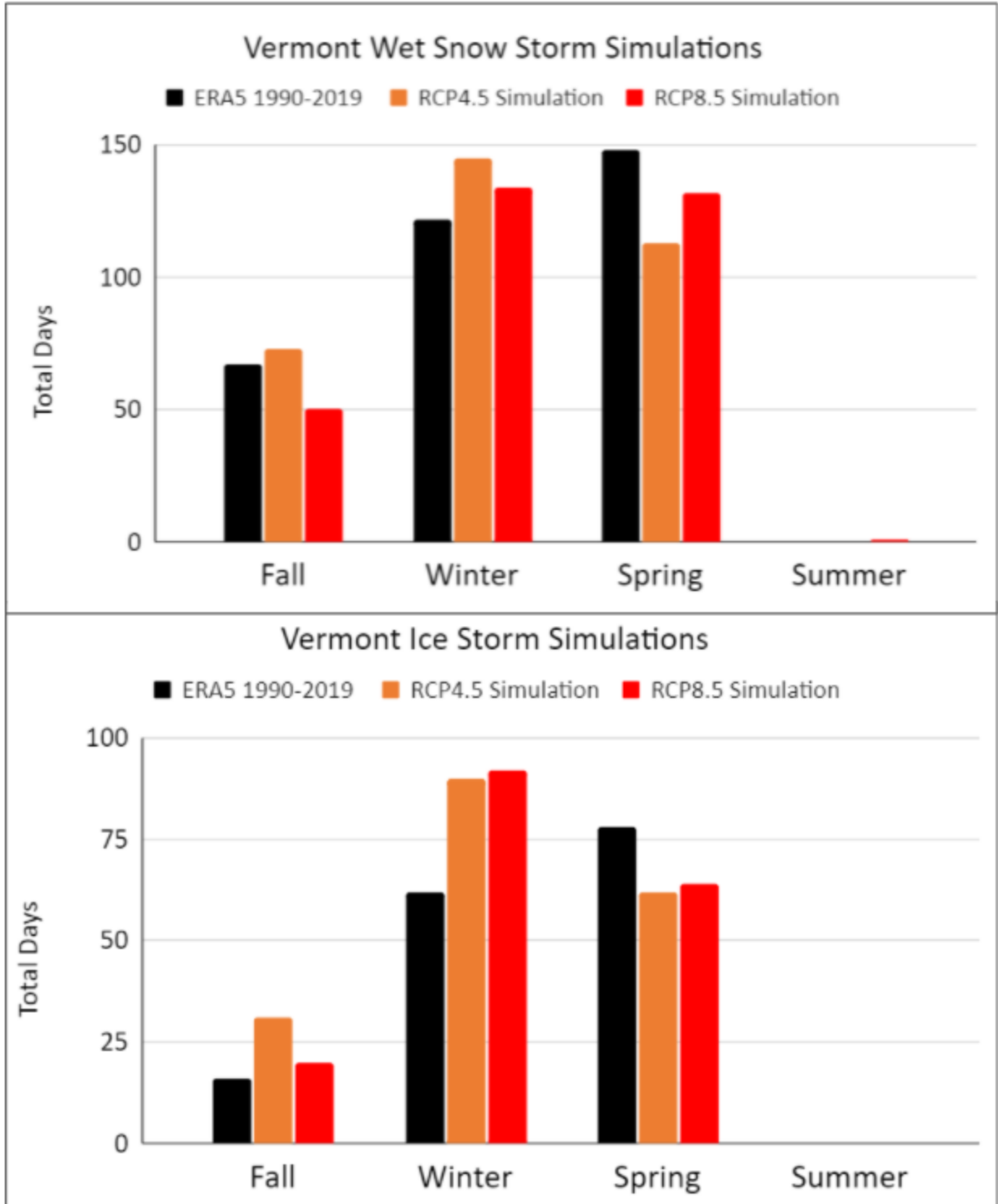


Figure 33. Climate simulations for significant wet snow and ice accumulation days from 2020 to 2049.

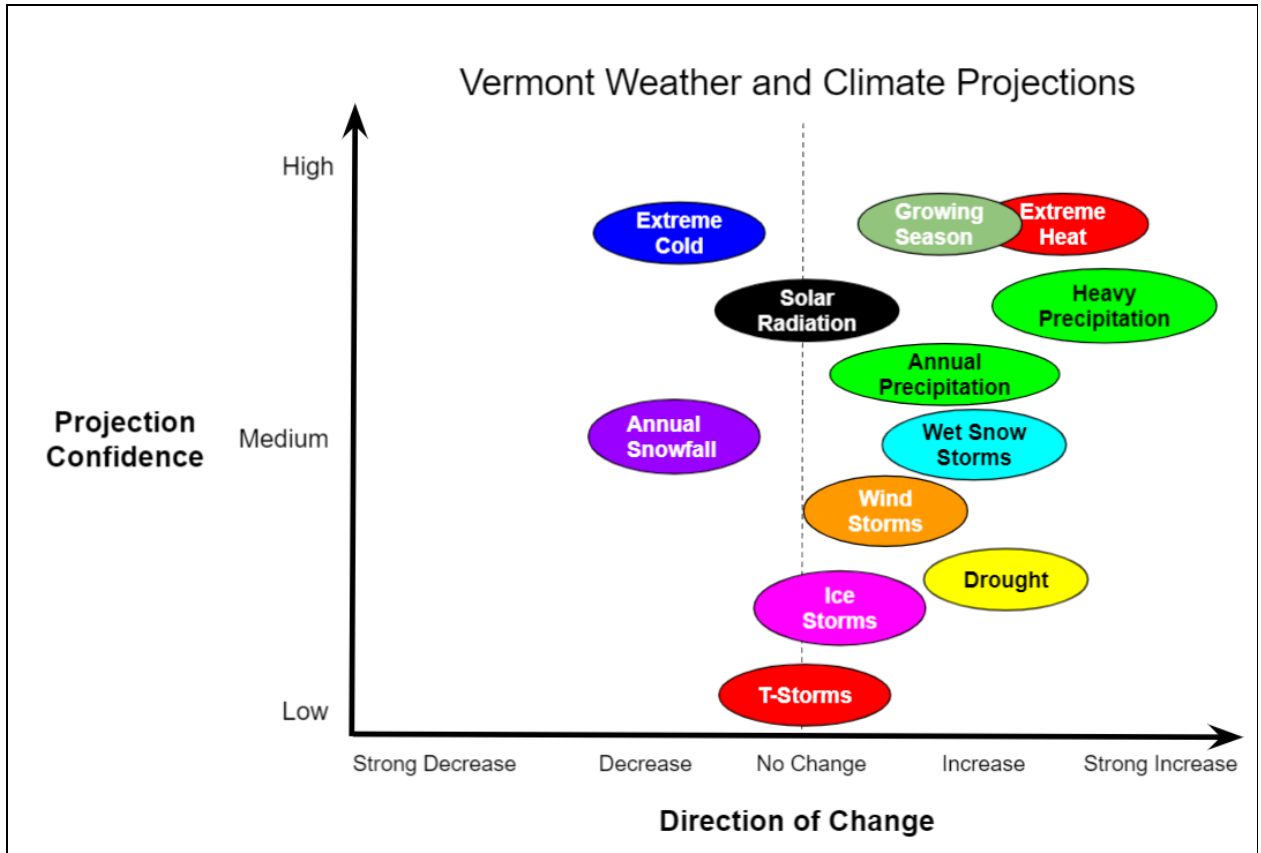


Figure 34. Vermont weather hazards and climate states directionality with projection confidence referenced from 1990-2019 to 2020-2049.

7. Summary and Conclusions

This report describes how climate change may present itself through the behavior of weather systems and climate states and how these collective changes may affect the reliable operation of VEC's assets through 2049. Overall risk to operating the electric grid does appear to increase primarily as a result of potentially more intense storm systems. Wind storms represent the greatest risk, with 68% of all weather-caused distribution system outages produced by wind that may cause tree conflicts within or from outside right of ways, or when extreme winds exceed rated design standards. Secondary risk factors such as wind direction and soil moisture were also examined, but given asynchronous effects and data limitations, this analysis was based primarily on one-variable synchronous impacts. Trends in power outage impacts show that the most severe storms have increased their outage impacts by 7% (1980-1990 vs. 2000-2019), and account for a large fraction of overall outage risk. An increase of distribution system power outages around +6% is projected with a moderate degree of confidence for VEC aggregated power outage risk through 2049 (1990-2019 to 2020-2049).

There is a high degree of confidence that Vermont's climate is warming and becoming wetter, both of which will likely continue to increase into the future. Warmer and wetter storm systems generally produce storms that are more intense (not necessarily more frequent). Seasonal changes to the warm season show a widening of the summer into early fall, which is expected to continue. This warm season widening will have the effect of lengthening the fall storm season into early winter (over 50% of all power outage impacts occur October to December). The most extreme storms (e.g., Superstorm Sandy, Tropical Storm Philippe extratropical transition) still appear most likely during the mid-fall season from approximately mid October to early November when the climatological nexus of tropical moisture and mid latitude temperature gradients creates significant energy for storm development. Widespread extreme precipitation and resulting flooding also peaks for these mid-fall storms when surface runoff is greater. Despite a warming winter, this work also shows that the winter season will remain cold enough to sustain and increase wet snow and ice storm risks through 2049. Midwinter will likely feature fewer quieter outage impact periods as a result of warmer winters.

The distribution system likely features slightly greater risk from low-frequency, high-impact storms as potential storm intensity increases; this more than likely would be from inland-tracking tropical storms or hurricanes. Given the low frequency of such extreme wind risks, however, it is difficult to determine the "storm intensity speed limit" of future storms as regulated by temperature increases and storm behavior changes.

Regarding peak load system management, more extreme high temperatures will tend to shift annual peak loads to summertime. Extreme cold will still occur but the distribution of temperatures will tend to grow to the right hand tail (heat extremes) faster and move slowly away from the left hand tail (cold extremes). Solar energy impacts from changes in incoming solar radiation did not appear to be significant when aggregated annually. However, seasonal changes of a warmer late summer and early fall period will likely produce sunnier conditions, resulting in midday behind-the-meter solar PV load minimums continuing well into the fall shoulder season. Annual yields of solar energy do not appear to vary significantly through 2049 from current year-to-year variability.

Heavy precipitation events are expected to continue to increase around twice as fast as annual precipitation. A higher frequency of heavy precipitation events may result in greater widespread flooding risks, especially during the fall season. More irregular precipitation patterns are also likely, potentially leading to more intense drought conditions. However, vegetation health and growth analysis show no clear or strong indications as to how precipitation changes may affect future tree health and growth. The availability of soil moisture will continue to be the most important control of seasonal tree growth. Future work could examine vegetation management applications, but the time and effort required to investigate this may yield limited results.

Information and insights provided within the report suggests that additional investments are likely needed to maintain reliability as the effects of climate change produce increased system risks. Increasing system resilience through more aggressive vegetation management, replacing aging infrastructure, and/or hardening existing assets may all be effective strategies in responding to climate change risks.

References

- Anderson, I., D. Rizzo, D. Huston, and M. Dewoolkar, 2017: Analysis of bridge and stream conditions of over 300 Vermont bridges damaged in Tropical Storm Irene. *Structure and Infrastructure Engineering*, 13, 1437-1450, doi:10.1080/15732479.2017.1285329.
- Bruyère, C. L., J. M. Done, G. J. Holland, and S. Fredrick, 2014: Bias corrections of global models for regional climate simulations of high-impact weather. *Clim. Dyn.*, 43, 1847–1856, <https://doi.org/10.1007/s00382-013-2011-6>.
- Bruyere, C. L., A. J. Monaghan, D. F. Steinhoff, and D. Yates, 2015: Bias-Corrected CMIP5 CESM Data in WRF/MPAS Intermediate File Format. <https://doi.org/http://dx.doi.org/10.5065/D6445JJ7>.
- Dudhia, J., 1989: Numerical Study of Convection Observed during the Winter Monsoon Experiment Using a Mesoscale Two-Dimensional Model. *J. Atmos. Sci.*, 46, 3077–3107, [https://doi.org/10.1175/1520-0469\(1989\)046<3077:NSOCOD>2.0.CO;2](https://doi.org/10.1175/1520-0469(1989)046<3077:NSOCOD>2.0.CO;2).
- Erlor, A. R., W. R. Peltier, M. D'Orgeville, A. R. Erlor, W. R. Peltier, and M. D'Orgeville, 2015: Dynamically Downscaled High-Resolution Hydroclimate Projections for Western Canada. *J. Clim.*, 28, 423–450, <https://doi.org/10.1175/JCLI-D-14-00174.1>.
- Erlor, A. R., W. R. Peltier, A. R. Erlor, and W. R. Peltier, 2016: Projected Changes in Precipitation Extremes for Western Canada based on High-Resolution Regional Climate Simulations. *J. Clim.*, 29, 8841–8863, <https://doi.org/10.1175/JCLI-D-15-0530.1>.
- Erlor, A. R., and Coauthors, 2019a: Simulating Climate Change Impacts on Surface Water Resources Within a Lake-Affected Region Using Regional Climate Projections. *Water Resour. Res.*, 55, 130–155, <https://doi.org/10.1029/2018WR024381>.
- Erlor, A. R., and Coauthors, 2019b: Evaluating Climate Change Impacts on Soil Moisture and Groundwater Resources Within a Lake-Affected Region. *Water Resour. Res.*, 55, 8142–8163, <https://doi.org/10.1029/2018WR023822>.
- Huang, H., J. Winter, E. Osterberg, R. Horton, and B. Beckage, 2017: Total and Extreme Precipitation Changes over the Northeastern United States. *Journal of Hydrometeorology*, 18, 1783-1798, doi:10.1175/jhm-d-16-0195.1.
- Keeling, Ralph and Tans, Pieter, 2021: Mauna Loa Observatory CO₂ Observations. National Oceanic and Atmospheric Administration/Global Monitoring Laboratory, assessed June 16 2021, <https://gml.noaa.gov/ccgg/trends/>.
- Leduc, M., and Coauthors, 2019: The ClimAx Project: A 50-Member Ensemble of Climate Change Projections at 12-km Resolution over Europe and Northeastern North America with the Canadian Regional Climate Model (CRCM5). *J. Appl. Meteorol. Climatol.*, 58, 663–693, <https://doi.org/10.1175/JAMC-D-18-0021.1>.

- Innocenti, S., and Coauthors, 2019: Observed and simulated precipitation over northeastern North America: how do daily and sub-daily extremes scale in space and time? *J. Clim.*, JCLI-D-19-0021.1, <https://doi.org/10.1175/JCLI-D-19-0021.1>.
- IPCC, 2018: Global warming of 1.5°C. An IPCC Special Report on the impacts of global warming of 1.5°C above pre-industrial levels and related global greenhouse gas emission pathways, in the context of strengthening the global response to the threat of climate change, sustainable development, and efforts to eradicate poverty [V. Masson-Delmotte, P. Zhai, H. O. Pörtner, D. Roberts, J. Skea, P.R. Shukla, A. Pirani, W. Moufouma-Okia, C. Péan, R. Pidcock, S. Connors, J. B. R. Matthews, Y. Chen, X. Zhou, M. I. Gomis, E. Lonnoy, T. Maycock, M. Tignor, T. Waterfield (eds.)]. In Press.
- Jiménez, P. A., J. Dudhia, J. F. González-Rouco, J. Navarro, J. P. Montávez, and E. García-Bustamante, 2012: A Revised Scheme for the WRF Surface Layer Formulation. *Mon. Weather Rev.*, 140, 898–918, <https://doi.org/10.1175/MWR-D-11-00056.1>.
- Kain, J. S., 2004: The Kain–Fritsch Convective Parameterization: An Update. *J. Appl. Meteorol.*, 43, 170–181, [https://doi.org/10.1175/1520-0450\(2004\)043<0170:TKCPAU>2.0.CO;2](https://doi.org/10.1175/1520-0450(2004)043<0170:TKCPAU>2.0.CO;2).
- Miller-Weeks, M., C. Eagar, and T. Petersen, 1999: The northeastern ice storm, 1998. NEFA, cooperating with the USDA Forest Service, [Durham, N.H.],.
- Mlawer, E. J., S. J. Taubman, P. D. Brown, M. J. Iacono, and S. A. Clough, 1997: Radiative transfer for inhomogeneous atmospheres: RRTM, a validated correlated-k model for the longwave. *J. Geophys. Res.*, 102, 16663, <https://doi.org/10.1029/97JD00237>.
- Panteli, M., and P. Mancarella, 2015: Influence of extreme weather and climate change on the resilience of power systems: Impacts and possible mitigation strategies. *Electric Power Systems Research*, 127, 259-270, doi:10.1016/j.epsr.2015.06.012.
- Peltier, W. R., M. d'Orgeville, A. R. Erler, F. Xie, W. R. Peltier, M. d'Orgeville, A. R. Erler, and F. Xie, 2018: Uncertainty in Future Summer Precipitation in the Laurentian Great Lakes Basin: Dynamical Downscaling and the Influence of Continental-Scale Processes on Regional Climate Change. *J. Clim.*, 31, 2651–2673, <https://doi.org/10.1175/JCLI-D-17-0416.1>.
- Perica, S., Pavlovic, S., St. Laurent M., Trypaluk, C., Unruh, D., Martin, D., and Wilhite, O. (2015, revised 2019). NOAA Atlas 14 Volume 10 Version 3, Precipitation-Frequency Atlas of the United States, Northeastern States. NOAA, National Weather Service, Silver Spring, MD.
- Pleim, J. E., 2007: A Combined Local and Nonlocal Closure Model for the Atmospheric Boundary Layer. Part I: Model Description and Testing. *J. Appl. Meteorol. Climatol.*, 46, 1383–1395, <https://doi.org/10.1175/JAM2539.1>.
- Rae, J., Y. Zhang, X. Liu, G. Foster, H. Stoll, and R. Whiteford, 2021: Atmospheric CO₂ over the Past 66 Million Years from Marine Archives. *Annual Review of Earth and Planetary Sciences*, 49, 609-641, doi:10.1146/annurev-earth-082420-063026.
- Salathé, E. P., and Coauthors, 2014: Estimates of Twenty-First-Century Flood Risk in the Pacific Northwest Based on Regional Climate Model Simulations. *J. Hydrometeorol.*, 15, 1881–1899, <https://doi.org/10.1175/JHM-D-13-0137.1>.

- Sanders, K., and B. Barjenbruch, 2016: Analysis of Ice-to-Liquid Ratios during Freezing Rain and the Development of an Ice Accumulation Model. *Weather and Forecasting*, 31, 1041-1060, doi:10.1175/waf-d-15-0118.1.
- Seneviratne, S.I., N. Nicholls, D. Easterling, C.M. Goodess, S. Kanae, J. Kossin, Y. Luo, J. Marengo, K. McInnes, M. Rahimi, M. Reichstein, A. Sorteberg, C. Vera, and X. Zhang, 2012: Changes in climate extremes and their impacts on the natural physical environment. In: *Managing the Risks of Extreme Events and Disasters to Advance Climate Change Adaptation* [Field, C.B., V. Barros, T.F. Stocker, D. Qin, D.J. Dokken, K.L. Ebi, M.D. Mastrandrea, K.J. Mach, G.-K. Plattner, S.K. Allen, M. Tignor, and P.M. Midgley (eds.)]. A Special Report of Working Groups I and II of the Intergovernmental Panel on Climate Change (IPCC). Cambridge University Press, Cambridge, UK, and New York, NY, USA, pp. 109-230.
- Siuta, D., G. West, and R. Stull, 2017: WRF hub-height wind forecast sensitivity to PBL scheme, grid length, and initial condition choice in complex terrain. *Weather Forecast.*, 32, <https://doi.org/10.1175/WAF-D-16-0120.1>.
- Skamarock, W. C., and Coauthors, 2019: A Description of the Advanced Research WRF Model Version 4. 1–162, <https://doi.org/10.5065/1dfh-6p97>.
- Swanston, C. et al., 2017: Vulnerability of forests of the Midwest and Northeast United States to climate change. *Climatic Change*, 146, 103-116, doi:10.1007/s10584-017-2065-2.
- Tewari, M., and Coauthors, 2004: Implementation and verification of the unified Noah land surface model in the WRF model. 20th Conf. on Weather Analysis and Forecasting/16th Conf. on Numerical Weather Prediction, Seattle, WA, American Meteorological Society.
- Thompson, G., P. R. Field, R. M. Rasmussen, and W. D. Hall, 2008: Explicit Forecasts of Winter Precipitation Using an Improved Bulk Microphysics Scheme. Part II: Implementation of a New Snow Parameterization. *Mon. Weather Rev.*, 136, 5095–5115, <https://doi.org/10.1175/2008MWR2387.1>.
- Thompson, G., 2013: High-resolution winter simulations of winter precipitation over the Colorado Rockies. Workshop on Parameterization of Clouds and Precipitation, Reading, UK, ECMWF <https://www.ecmwf.int/node/12672>.
- USGCRP, 2018: Impacts, Risks, and Adaptation in the United States: Fourth National Climate Assessment, Volume II [Reidmiller, D.R., C.W. Avery, D.R. Easterling, K.E. Kunkel, K.L.M. Lewis, T.K. Maycock, and B.C. Stewart (eds.)]. U.S. Global Change Research Program, Washington, DC, USA, 1515 pp. doi: 10.7930/NCA4.2018.
- Van Houtven, G., J. Phelan, C. Clark, R. Sabo, J. Buckley, R. Thomas, K. Horn, and S. LeDuc, 2019: Nitrogen deposition and climate change effects on tree species composition and ecosystem services for a forest cohort. *Ecological Monographs*, 89, e01345, doi:10.1002/ecm.1345.
- Vermont Emergency Management, Department of Public Safety, 2018: 2018 Vermont State Hazard Mitigation Plan.

Wang, W., H. He, F. Thompson, J. Fraser, and W. Dijk, 2016: Changes in forest biomass and tree species distribution under climate change in the northeastern United States. *Landscape Ecology*, 32, 1399-1413, doi:10.1007/s10980-016-0429-z.